

**Atmospheric water
vapour tracers**

H. F. Goessling and
C. H. Reick

Atmospheric water vapour tracers and the significance of the vertical dimension

H. F. Goessling^{1,2,*} and C. H. Reick¹

¹Max Planck Institute for Meteorology, Hamburg, Germany

²International Max Planck Research School on Earth System Modelling, Hamburg, Germany

*now at: Alfred Wegener Institute for Polar and Marine Research, Bremerhaven, Germany

Received: 15 September 2012 – Accepted: 6 November 2012 – Published: 22 November 2012

Correspondence to: H. F. Goessling (helge.goessling@awi.de)

Published by Copernicus Publications on behalf of the European Geosciences Union.

Title Page

Abstract

Introduction

Conclusions

References

Tables

Figures

⏪

⏩

◀

▶

Back

Close

Full Screen / Esc

Printer-friendly Version

Interactive Discussion



Abstract

Atmospheric water vapour tracers (WVTs) are an elegant tool to determine source-sink relations of moisture “online” in atmospheric general circulation models (AGCMs). However, it is sometimes desirable to establish such relations “offline” based on already existing atmospheric data (e.g. reanalysis data). One simple and frequently applied offline method is 2-D moisture tracing. It makes use of the “well-mixed” assumption, which allows to treat the vertical dimension integratively.

Here we scrutinise the “well-mixed” assumption and 2-D moisture tracing by means of analytical considerations in combination with AGCM-WVT simulations. We find that vertically well-mixed conditions are seldomly met. Due to the presence of vertical inhomogeneities, 2-D moisture tracing (I) neglects a significant degree of fast-recycling, and (II) results in erroneous advection where the direction of the horizontal winds varies vertically. The latter is not so much the case in the extratropics, but in the tropics this can lead to large errors. For example, computed by 2-D moisture tracing, the fraction of precipitation in the Western Sahel that originates from beyond the Sahara is ~ 40 %, whereas the fraction that originates from the tropical and Southern Atlantic is only ~ 4 %. Full (i.e. 3-D) moisture tracing however shows that both regions contribute roughly equally, which reveals the results of an earlier study as spurious.

Moreover, we point out that there are subtle degrees of freedom associated with the implementation of WVTs into AGCMs because the strength of mixing between precipitation and the ambient water vapour is not completely provided by such models. We compute an upper bound for the resulting uncertainty and show that this uncertainty is smaller than the errors associated with 2-D moisture tracing.

1 Introduction

Source-sink relations of atmospheric moisture characterise the Earth’s hydrological cycle. They have been used for example to investigate the cause of extreme precipitation

ACPD

12, 30119–30176, 2012

Atmospheric water vapour tracers

H. F. Goessling and
C. H. Reick

Title Page

Abstract

Introduction

Conclusions

References

Tables

Figures

⏪

⏩

◀

▶

Back

Close

Full Screen / Esc

Printer-friendly Version

Interactive Discussion



Atmospheric water vapour tracersH. F. Goessling and
C. H. Reick

Title Page

Abstract

Introduction

Conclusions

References

Tables

Figures

◀

▶

◀

▶

Back

Close

Full Screen / Esc

Printer-friendly Version

Interactive Discussion



events (e.g. Sodemann et al., 2009) and to estimate to what extent precipitation is sustained by continental moisture recycling (e.g. van der Ent et al., 2010). Source-sink relations of atmospheric moisture are considered to contain information on how strongly precipitation somewhere is causally linked to evaporation elsewhere, though the conclusiveness of source-sink relations to establish causalities is not beyond controversy (Goessling and Reick, 2011). Nevertheless, knowledge about the paths moisture takes in the atmosphere is believed to be associated with at least some predictive skill, for example regarding the impact potential land-use changes may have on precipitation patterns.

By measuring the ratios of stable water isotopes in precipitation (e.g. Dansgaard, 1964; Salati et al., 1979), one can retrieve only vague information on where the water has evaporated; the few degrees of freedom that are associated with the stable-isotope composition do not allow for the determination of a reasonably resolved spatial pattern of the evaporative sources. To determine the latter one has to recur to numerical tracing of moisture, which can be realised either offline, i.e. a posteriori, using suitable data on evaporation, precipitation, and atmospheric transport, or online within an atmospheric general circulation model (AGCM).

Online moisture tracing was first applied by Koster et al. (1986) and Joussaume et al. (1986). In this context, Bosilovich (2002) coined the term *passive water vapour tracers* (WVTs), where passive means that the AGCM's prognostic variables are not affected by the WVTs (see also Bosilovich and Schubert, 2002; Bosilovich et al., 2002). Online tracing offers the advantage that any variables characterising the atmospheric state are available at the AGCM's temporal and spatial resolution, including the vertical dimension. Disadvantages of online tracing are that (I) AGCMs not constrained by data assimilation can not reproduce particular real-world situations but only reflect the Earth's long-term climate, including inevitable biases, and that (II) to determine the fate of the moisture evaporated from each predefined set of source regions one has to run the whole computationally expensive AGCM.

Atmospheric water vapour tracers

H. F. Goessling and
C. H. Reick

[Title Page](#)[Abstract](#)[Introduction](#)[Conclusions](#)[References](#)[Tables](#)[Figures](#)[◀](#)[▶](#)[◀](#)[▶](#)[Back](#)[Close](#)[Full Screen / Esc](#)[Printer-friendly Version](#)[Interactive Discussion](#)

By contrast, offline moisture tracing is computationally less expensive and can be applied to different kinds of data including reanalyses that arguably constitute the best guess of the evolution of the global atmospheric state during recent decades. While the generation of reanalyses involves AGCMs, the stored output data typically do neither contain all atmospheric state variables that are needed to perform a full 3-D tracing comparable to the online tracing, nor is their spatio-temporal resolution as high as in case of the online tracing. While the large-scale flow field is usually sufficiently characterised by reanalysis data, the processes that cause vertical redistribution of moisture – turbulent diffusion and precipitation – are usually not sufficiently characterised.

Several offline moisture tracing techniques have been developed that cope with the limitations of reanalysis-like data. Among these are sophisticated approaches like the Lagrangian particle dispersion method (e.g. Stohl and James, 2004) and the quasi-isentropic back-trajectory method (e.g. Dirmeyer and Brubaker, 1999), but also the conceptually simpler approach of 2-D moisture tracing (Yoshimura et al., 2004; van der Ent et al., 2010; van der Ent and Savenije, 2011; Goessling and Reick, 2011; Keys et al., 2012). In the latter case the atmospheric fields are integrated vertically before the tracing is then performed only in the horizontal dimensions.

2-D moisture tracing has been applied to estimate continental precipitation recycling ratios (i.e. the (spatially resolved) fraction of precipitation that stems from continental evaporation; Yoshimura et al., 2004; van der Ent et al., 2010; Goessling and Reick, 2011) and continental evaporation recycling ratios (i.e. the (spatially resolved) fraction of evaporation that precipitates on land; van der Ent et al., 2010), but has also been used to determine source-sink relations at geographically smaller scales. Recently, Keys et al. (2012) used 2-D moisture tracing to determine what they call the precipitationsheds of certain regions supposed to be particularly vulnerable to changes in precipitation. For the Western Sahel, Keys et al. (2012) found that the mediterranean and adjacent regions contribute substantially to the region's growing-season precipitation, while relatively small amounts of moisture are advected from the tropical Atlantic Ocean (Fig. 3 in Keys et al., 2012).

**Atmospheric water
vapour tracers**H. F. Goessling and
C. H. Reick

Title Page

Abstract

Introduction

Conclusions

References

Tables

Figures

◀

▶

◀

▶

Back

Close

Full Screen / Esc

Printer-friendly Version

Interactive Discussion



However, we have argued earlier (Goessling and Reick, 2011) that 2-D moisture tracing may produce large errors particularly in tropical and subtropical Western Africa because of the meteorological situation prevailing there in summer: while in the monsoonal layer below 750 hPa moisture is advected from the tropical Atlantic, the African Easterly Jet above 750 hPa carries moisture from the east and the north. In this study we therefore put one focus on the Western Sahel.

The theoretical basis of 2-D moisture tracing is the so-called “well-mixed” assumption: the fractions of moisture stemming from different evaporative source regions in total atmospheric moisture are assumed to be independent of height. The “well-mixed” assumption has a long history and was first used in the context of simple, regionally applied recycling models (e.g. Budyko, 1974; Brubaker et al., 1993; Eltahir and Bras, 1994). These recycling models included further simplifications that were associated with averaging over other dimensions. Put in context to these simpler recycling models, 2-D moisture tracing is the least simplifying method that still invokes the “well-mixed” assumption for the vertical dimension – all other dimensions (the horizontal space dimensions and the time dimension) are explicitly resolved. It seems worth to mention that there are also attempts to relax the “well-mixed” assumption while keeping simplifications regarding the other dimensions (e.g. Burde, 2006; Fitzmaurice, 2007).

To investigate the validity of the “well-mixed” assumption, Bosilovich (2002) traced moisture from different source regions located in North America using an AGCM equipped with WVTs. Bosilovich (2002) found that the moisture stemming from these regions tends to be inhomogeneously distributed vertically, with moisture of local origin being enriched in low levels. In one part of our study we further investigate the validity of the “well-mixed” assumption using basically the same methodology as Bosilovich (2002). However, we also quantify the errors that arise from the 2-D approximation by comparing source-sink relations of atmospheric moisture as determined by 2-D and 3-D moisture tracing.

It turns out, however, that the online 3-D moisture tracing itself, which we use as reference, bears some uncertainty in the way it is implemented: while the net exchange

Atmospheric water vapour tracersH. F. Goessling and
C. H. Reick

Title Page

Abstract

Introduction

Conclusions

References

Tables

Figures

◀

▶

◀

▶

Back

Close

Full Screen / Esc

Printer-friendly Version

Interactive Discussion



of water molecules between falling rain drops and the ambient air is part of an AGCM's implementation, assumptions have to be made regarding the degree to which gross evaporation and gross condensation act to mix the precipitation with the ambient water vapour. Instead of trying to come up with one single implementation that is as close as possible to reality – which is a non-trivial task (see Sect. 8) –, we implemented two different 3-D moisture tracing variants that span the range of possible behaviour: in one case precipitation is assumed to mix instantaneously with the ambient water vapour (strong mixing), and in another case it is assumed that only the net exchange of water between precipitation and air takes place (weak mixing). This allows us to estimate the maximum uncertainty associated with this issue.

The paper is structured as follows. In Sect. 2 we set forth the theoretical basis of the 2-D approximation and show that 2-D tracing is exact under vertically well-mixed conditions. In Sect. 3 we present characteristics of the atmosphere that determine whether the atmosphere is well-mixed or not. These characteristics hence strongly influence the accuracy of the 2-D approximation. We then describe the implementation of WVTs into the AGCM ECHAM6 in Sect. 4.1, followed by a short validation of the WVT scheme in Sect. 4.2. In Sect. 5 we investigate to what extent the “well-mixed” assumption holds according to our simulations. Subsequently, we quantify in Sect. 6 the maximum uncertainty of 3-D moisture tracing that is related to the question of how strongly precipitation mixes with the ambient water vapour. In Sect. 7 we compare results obtained by 2-D moisture tracing with results obtained by 3-D moisture tracing. Finally, we discuss limitations and further aspects in Sect. 8 and draw conclusions in Sect. 9.

2 The theoretical basis of 2-D moisture tracing

In this section we discuss the theoretical basis of the 2-D approximation and demonstrate that 2-D moisture tracing is exact – where we mean “identical to 3-D moisture tracing” – if the “well-mixed” assumption is valid. We demonstrate that well-mixed

conditions are necessary for 2-D moisture tracing to be exact for two reasons. The first concerns the question from which height precipitation is drawn, and the second relates to the impact of wind shear on horizontal moisture advection.

The “well-mixed” assumption implies that water molecules of different origin are perfectly mixed in the vertical dimension, i.e. that the fraction f_i of any WVT species i in total moisture is independent of height z (m):

$$f_i(z) = \frac{q_i(z)}{q(z)} \stackrel{!}{=} \hat{f}_i \quad \forall z \quad (1)$$

where q_i (kg kg^{-1}) is the specific concentration of moisture stemming from the source region i , q (kg kg^{-1}) is the total specific moisture for which it holds that $q = \sum_i q_i$, and

$$\hat{f}_i = \frac{\hat{q}_i}{\hat{q}} \quad (2)$$

with

$$\hat{q}_i = \int_0^{\infty} \rho q_i \, dz \quad (3)$$

and

$$\hat{q} = \int_0^{\infty} \rho q \, dz \quad (4)$$

where ρ (kg m^{-3}) is the air density. Here and in the following we simplify the notation inside integrals by dropping the argument that indicates the dependency of the variables on z (a notation that we adopt also for the other spatio-temporal dimensions).

Atmospheric water vapour tracers

H. F. Goessling and
C. H. Reick

Title Page

Abstract

Introduction

Conclusions

References

Tables

Figures

◀

▶

◀

▶

Back

Close

Full Screen / Esc

Printer-friendly Version

Interactive Discussion



Discussion Paper | Discussion Paper | Discussion Paper | Discussion Paper

If the “well-mixed” assumption (Eq. 1) does not hold, the composition of precipitation P arriving at the surface depends on the height from which the moisture originates:

$$\frac{P_i}{P} = \frac{\int_0^\infty f_i p^* dz}{\int_0^\infty p^* dz} \quad (5)$$

5 where P_i (kg m^{-2}) is the amount of precipitation that stems from the source region i and $p^*(z)dz$ (kg m^{-2}) is the amount of precipitation drawn from the height z . It is obvious that p^* can be interpreted as a vertical weight function. Note, however, that p^* is not simply the (vertically resolved) difference of condensation and re-evaporation, but the result of a downward propagating integrative process that involves additional
10 assumptions regarding the gross terms of condensation and evaporation, see below. Only if the “well-mixed” assumption (Eq. 1) holds, Eq. (5) becomes $P_i/P = \hat{f}_i$, i.e. the vertical dimension does not need to be resolved to correctly determine the composition of precipitation.

We now turn to the second reason why 2-D moisture tracing requires well-mixed
15 conditions to be exact, which concerns horizontal advection. To this end we start from the full 3-D transport (advection) equation, and derive the 2-D formulation by vertical integration. For the sake of simplicity we omit one of the two horizontal dimensions. The full transport equation for a WVT species i without sources and sinks reads

$$\frac{\partial(\rho q_i)}{\partial t} + \frac{\partial(\rho q_i u)}{\partial x} + \frac{\partial(\rho q_i w)}{\partial z} = 0 \quad (6)$$

20 where u (m s^{-1}) is the wind speed along the horizontal dimension x (m), and w (m s^{-1}) is the wind speed along the vertical dimension. As a side remark, in large-scale AGCMs the vertical term can only partly be handled explicitly because subgrid-scale processes (“turbulent diffusion”) typically dominate the vertical transport. Turbulent (convective)
25 processes are therefore handled by additional parameterisations.

Atmospheric water vapour tracers

H. F. Goessling and
C. H. Reick

Title Page

Abstract

Introduction

Conclusions

References

Tables

Figures

◀

▶

◀

▶

Back

Close

Full Screen / Esc

Printer-friendly Version

Interactive Discussion



Vertical integration of Eq. (6) gives

$$\int_0^{\infty} \frac{\partial(\rho q_i)}{\partial t} dz + \int_0^{\infty} \frac{\partial(\rho q_i u)}{\partial x} dz = 0. \quad (7)$$

The integral of the vertical term in Eq. (6) is zero because $w = 0$ for $z = 0$ and $\rho \rightarrow 0$ for $z \rightarrow \infty$. Equation (7) can be rewritten as

$$\frac{\partial \hat{q}_i}{\partial t} + \frac{\partial \hat{q}_i \hat{u}_i}{\partial x} = 0 \quad (8)$$

with

$$\hat{u}_i = \frac{\int_0^{\infty} \rho q f_i u dz}{\int_0^{\infty} \rho q f_i dz}. \quad (9)$$

Here, \hat{u}_i is a tracer-density-weighted vertical average of the horizontal wind speed, and multiplication of \hat{u}_i with the vertically integrated tracer mass \hat{q}_i gives the vertically integrated horizontal flux of the WVT species i . \hat{u}_i can thus be interpreted as an effective wind speed at which the WVT species i is horizontally advected.

If f_i varies with height, \hat{u}_i is generally different for different tracer species i . If, however, the “well-mixed” assumption holds, f_i drops out of Eq. (9) and, hence, \hat{u}_i becomes the WVT-species independent effective wind speed \hat{u} :

$$\hat{u}_i = \hat{u} = \frac{\int_0^{\infty} \rho q u dz}{\int_0^{\infty} \rho q dz} \quad \forall i \quad (10)$$

which leads to the horizontal advection equation of the 2-D approximation:

$$\frac{\partial \hat{q}_i}{\partial t} + \frac{\partial \hat{q}_i \hat{u}}{\partial x} = 0. \quad (11)$$

This relation is exact if f_i is independent of height, i.e. if the “well-mixed” assumption holds (Eq. 1).

Equation (9) further reveals that $\hat{u}_i = \hat{u} \forall i$ also if the horizontal winds are not sheared vertically, meaning that in this case the 2-D-approximated horizontal advection term is exact irrespective of the validity of the “well-mixed” assumption. However, without well-mixed conditions the determination of the composition of precipitation would still require vertically resolved tracer fields (see above).

In summary, the results of the above considerations are:

- If the atmospheric moisture is perfectly well-mixed vertically, the 2-D approximation is exact. This is true even if the horizontal winds are sheared vertically.
- If the atmospheric moisture is not well-mixed but the horizontal winds are vertically uniform, the 2-D advection term is exact. However, in this case the composition of precipitation can not be determined exactly without resolving the vertical dimension.

Of course in reality the atmosphere is not perfectly well-mixed vertically, and the horizontal winds are not uniform vertically. However, the above analysis reveals that the size of errors introduced by 2-D moisture tracing must depend on the degree to which atmospheric conditions deviate from these limit cases. Therefore, we investigate in the next section key characteristics of the atmosphere that largely influence the above mentioned factors, and analyse in Sect. 5 to what extent 3-dimensionally simulated atmospheric conditions deviate from well-mixed conditions.

3 Relevant characteristics of the atmosphere

The numerical simulations we investigate in this paper are generated with ECHAM6 (Roeckner et al., 2003), the atmosphere-land component of the Max Planck Institute for Meteorology’s Earth system model (MPI-ESM), at T63/L47 resolution ($1.875^\circ \times 1.875^\circ$,

Atmospheric water vapour tracers

H. F. Goessling and
C. H. Reick

Title Page

Abstract

Introduction

Conclusions

References

Tables

Figures

⏪

⏩

◀

▶

Back

Close

Full Screen / Esc

Printer-friendly Version

Interactive Discussion



47 levels, 10 min time-step) with prescribed climatological sea-surface temperatures (SSTs) representing present-day conditions without interannual variability. In physical terms, all model experiments are binary identical (see the last paragraph of Sect. 4.1) and only the passive tracers behave differently between the experiments. The simulated patterns of precipitation and evaporation, averaged over 10 yr of equilibrated climate as all results shown in the following, are depicted in Fig. 1.

The basic assumption behind 2-D moisture tracing is the “well-mixed” assumption: atmospheric moisture is assumed to mix rapidly in the vertical dimension, resulting in a vertically uniform composition of the moisture column with respect to the moisture’s evaporative origin. In Sect. 2 we showed analytically that 2-D moisture tracing is exact under well-mixed conditions. Whether the atmosphere is well-mixed vertically or not results from the interplay between the generation of vertical inhomogeneities on the one hand and the strength of vertical mixing on the other hand. In this section we discuss the key mechanisms that lead to vertical inhomogeneities and, hence, to inaccuracies associated with 2-D moisture tracing.

First we consider the strength of vertical mixing. The lowest ~ 1000 m of air constituting the atmospheric boundary layer are typically continuously mixed by turbulent motions due to surface friction and dry convection. In contrast, the free troposphere above experiences rather sporadic mixing through the action of deep moist convection. While the relatively warm and hence moist boundary layer usually contains the bulk of the atmospheric moisture, the higher wind speeds in the free troposphere above have the effect that the free troposphere considerably contributes to the horizontal moisture flux. This suggests that the frequency of strong moist convective events may be a useful indicator for the degree of vertical mixing. We define moist convective events to be strong if the daily amount of convective precipitation exceeds 10 % of the total vertically integrated atmospheric water content, where the latter is averaged over the respective day (Fig. 2).

Strong moist convection occurs frequently in the tropical rain belt, which shifts its position during the course of the year, and in the extratropical stormtrack regions (Fig. 2).

Atmospheric water vapour tracersH. F. Goessling and
C. H. Reick

Title Page

Abstract

Introduction

Conclusions

References

Tables

Figures

◀

▶

◀

▶

Back

Close

Full Screen / Esc

Printer-friendly Version

Interactive Discussion



**Atmospheric water
vapour tracers**H. F. Goessling and
C. H. Reick

Title Page

Abstract

Introduction

Conclusions

References

Tables

Figures

◀

▶

◀

▶

Back

Close

Full Screen / Esc

Printer-friendly Version

Interactive Discussion



In the latter the signal is strongly seasonal: over the ocean, the frequency of strong moist convection is much higher during the respective hemisphere's winter, i.e. when the stormtracks are more pronounced. In contrast, over the northern extratropical continents strong moist convection is more frequent in northern summer. These patterns indicate qualitatively when and where vertical inhomogeneities with respect to moisture composition can be expected to relax quickly towards well-mixed conditions. Of course it is not only the strength of vertical mixing, but also the degree to which inhomogeneities are generated in the first place that determines whether the atmosphere attains an approximately well-mixed state. In the following we consider two factors that are responsible for the generation of vertical inhomogeneities.

First, vertical inhomogeneities with respect to moisture composition are generated by surface evaporation (Fig. 1, bottom) which acts to enrich moisture of local origin in the lower part of the atmosphere. One may consider surface evaporation as the primary cause of vertical inhomogeneities. Second, vertical inhomogeneities can be generated by advection if the horizontal winds are sheared vertically. This mechanism may be considered as a secondary cause of vertical inhomogeneities because it generates vertical inhomogeneities out of horizontal inhomogeneities. If the horizontal winds are sheared vertically, the composition of different layers in the atmosphere can be very different, in particular if vertical mixing is weak.

An idea to what extent the winds are sheared vertically can be obtained by comparing monthly means of the near-surface (925 hPa) winds and the mid-tropospheric (650 hPa) winds (Fig. 3, top and middle). For a more quantitative assessment one also has to take into account that the specific humidity of the air decreases steeply with height due to the temperature gradient, meaning that the same windspeed is associated with stronger moisture transport in lower levels than in higher levels.

It stands to reason that directional shear of the horizontal wind is more effective in generating vertical inhomogeneities than speed shear of the horizontal wind; in case of vertically uniform wind directions but varying wind speeds, a relatively low degree of vertical mixing may suffice to maintain close to well-mixed conditions. We therefore

introduce a measure Γ that quantifies the degree to which shear generates vertical inhomogeneities as follows:

$$\Gamma := \frac{\left\| \int_0^{\infty} \rho q \begin{pmatrix} u \\ v \end{pmatrix} dz \right\|}{\int_0^{\infty} \left\| \rho q \begin{pmatrix} u \\ v \end{pmatrix} \right\| dz} \quad (12)$$

where z is geometrical height, ρ is air density, q is specific humidity, u and v are the zonal and the meridional component of the horizontal wind, and $\|\cdot\|$ is the Euclidean norm. While the numerator is proportional to the absolute value of the vertically integrated horizontal moisture flux (Fig. 3, bottom), the denominator is proportional to what this flux would be if the winds at all heights pointed in the same direction (with the same orientation). Obviously, $\Gamma \in [0, 1]$, with low values indicating strong directional shear of the horizontal moisture flux and high values indicating weak directional shear of the horizontal moisture flux. In the following we refer to Γ simply as directional shear.

Γ (computed for 6-hourly data) reveals that strong directional shear is mostly confined to the tropics (Fig. 4). This is due to the fact that the weak Coriolis force near the equator allows the development of thermally direct circulations, while in the extratropics the Coriolis force acts to establish flow in approximate geostrophic balance, leading to vertically more uniform wind directions. Another striking feature is that strong directional shear often occurs at continental coasts, for example at the South American and African western coasts both in January and in July, and in a band ranging from the Gulf of Oman over India and Indochina to the Philippine Sea in January. This feature supports the supposition that directional shear is mainly caused by thermally direct circulations, because the latter are typically strongest in the vicinity of continental coasts.

Atmospheric water vapour tracers

H. F. Goessling and
C. H. Reick

Title Page

Abstract

Introduction

Conclusions

References

Tables

Figures



Back

Close

Full Screen / Esc

Printer-friendly Version

Interactive Discussion



Considered together, the frequency of strong moist convection (Fig. 2) and the magnitude of directional shear (Fig. 4) provide a qualitative idea of when and where the atmosphere may attain close to vertically well-mixed conditions, meaning that 2-D moisture tracing may be an appropriate approximation. However, a precise quantification of the errors that are introduced by vertical integration can only be obtained by direct comparison of results from 2-D and 3-D moisture tracing. We provide such a comparison in Sect. 7, where we come back to the quantities discussed in this section to explain the simulated differences.

4 Atmospheric water vapour tracers in ECHAM6

4.1 Implementation

Passive tracers in ECHAM6 (Roeckner et al., 2003) are horizontally advected with a flux-form semi-Lagrangian scheme introduced by Lin and Rood (1996). Vertical diffusion of tracers is implemented with the eddy diffusion method where the diffusivity is parameterised in terms of the turbulent kinetic energy (e.g. Garratt, 1992). Vertical redistribution of tracers is also caused by moist convection which is implemented in ECHAM6 with a Tiedtke-Nordeng scheme (Tiedtke, 1989; Nordeng, 1994). No horizontal diffusion is applied to tracers.

In addition to being transported as a passive tracer, atmospheric moisture is redistributed vertically by precipitation, which acts to keep water concentrations in higher levels low. Within an AGCM the vertically resolved precipitation fluxes can in principle be taken directly from the AGCM's internal (prognostic) variables. However, due to numerical issues related to the implementation of the flux-form advection scheme (Jöckel et al., 2001) and also due the moist convective parameterisation, ECHAM6 is not completely conserving water mass. We therefore decided to use an alternative method to diagnose the vertically resolved precipitation fluxes. This method ensures that the model's prognostic moisture is permanently equal to the sum over all WVTs.

Atmospheric water vapour tracers

H. F. Goessling and
C. H. Reick

Title Page

Abstract

Introduction

Conclusions

References

Tables

Figures



Back

Close

Full Screen / Esc

Printer-friendly Version

Interactive Discussion



In this approach the vertically resolved precipitation flux is diagnosed every time-step by comparing the model's internal (prognostic) moisture q_{prog} with the not yet precipitation-corrected sum over all WVT species

$$q_{\text{wvt}}(z) = \sum_{i=1}^N q_i(z) \quad (13)$$

where N is the number of WVTs and q_i is the specific concentration (kg kg^{-1}) of tracer i . For the method to be valid, any sources of atmospheric moisture as well as the atmosphere's initial moisture must be covered by one of the WVT species.

To avert obscurities, it seems advisable to give a comment on the terms gross and net that we use in the following. Gross re-evaporation and gross condensation account for all water molecules that cross the interface between the liquid (or solid) phase and the gaseous phase (i.e. the air). Considering for example air that is in contact with liquid water, and assuming that the air is saturated with respect to water vapour, gross re-evaporation and gross condensation take place at the same rate $R = C$. In consequence, net condensation $C - R$ (which is always equal to -1 times net re-evaporation) is zero. In fact, gross evaporation is generally not a function of the air's humidity, but only of the interface temperature because the latter determines the frequency at which water molecules heading towards the air are fast enough to overcome the attractive force exerted by the adjacent water molecules. Given a fixed interface temperature, the dependence of net evaporation/condensation on the air's humidity results only from the dependence of the gross condensation term on the air's humidity (for a detailed discussion see Silberberg et al., 1996).

The procedure described in the following is applied at the end of every model time-step and adjusts the sum over all WVTs q_{wvt} to the model's prognostic moisture q_{prog} ($= q$). Having thus started identically, after one model time-step without provision for vertical transport by precipitation, q_{wvt} is larger than q_{prog} if the local balance of gross condensation minus gross evaporation ($C - R$, ($\text{kg kg}^{-1} \text{s}^{-1}$)) is positive. This is the

**Atmospheric water
vapour tracers**H. F. Goessling and
C. H. Reick

Title Page

Abstract

Introduction

Conclusions

References

Tables

Figures

◀

▶

◀

▶

Back

Close

Full Screen / Esc

Printer-friendly Version

Interactive Discussion



case if net moisture is removed from the air at cost of an increasing downward precipitation flux. On the other hand, q_{wvt} is smaller than q_{prog} if $C - R$ is negative. This is the case if moisture is added to the air by net re-evaporation of precipitation. It is

$$(C - R)(z) = \frac{q_{\text{wvt}}(z) - q_{\text{prog}}(z)}{\Delta t} \quad (14)$$

where Δt (s) is the time-step length. One obtains the vertically resolved precipitation flux $P(z)$ ($\text{kg} (\text{m}^2 \text{s})^{-1}$) for the considered time-step at any height by integrating $C - R$ from the respective height to the top of the atmosphere:

$$P(z) = \int_z^{\infty} (C - R)(z') \rho(z') dz' . \quad (15)$$

Analogously to Eqs. (14) and (15), it holds for single WVT species that the change due to precipitation within the considered time-step is

$$\frac{\Delta q_i(z)}{\Delta t} = (C_i - R_i)(z) \quad (16)$$

and that

$$P_i(z) = \int_z^{\infty} (C_i - R_i)(z') \rho(z') dz' . \quad (17)$$

However, while $(C - R)$ is known (Eq. 14), $(C_i - R_i)$ is unknown. For the gross terms C_i and R_i we know that

$$C_i(z) = \frac{q_i(z)}{q_{\text{wvt}}(z)} C(z) \quad (18)$$

Atmospheric water vapour tracers

H. F. Goessling and
C. H. Reick

Title Page

Abstract

Introduction

Conclusions

References

Tables

Figures

◀

▶

◀

▶

Back

Close

Full Screen / Esc

Printer-friendly Version

Interactive Discussion



and

$$R_i(z) = \frac{P_i(z)}{P(z)} R(z). \quad (19)$$

If C and R are known individually, Eqs. (17)–(19) constitute a closed system of equations and can be solved proceeding from the top of the atmosphere downward, allowing to derive the change of each individual tracer species (Eq. 16). Adding these changes to the tracer concentrations q_i gives the precipitation corrected values $q_i^{\text{corr}} = q_i + \Delta q_i$, so that by Eqs. (13) and (14) $q_{\text{wvt}}^{\text{corr}} = q_{\text{prog}}$. Setting $q_i := q_i^{\text{corr}}$ at the end of the procedure hence ensures that q_{wvt} and q_{prog} start identically into the next time-step, which is necessary for the validity of our method.

However, C and R are not known individually, but only $C - R$ (Eq. 14), leaving Eqs. (17)–(19) underdetermined. Notably, this problem is not specific to our approach in which $C - R$ is diagnosed from the differences between q_{wvt} and q_{prog} (Eq. 14). AGCMs themselves operate only with the net term $C - R$ because the gross terms are not relevant for the physical system, i.e. the total water mass and energy balance. Hence, additional assumptions have to be made regarding the gross terms C and R in order to close the above system of equations.

One possible way to proceed would be to estimate realistic values of the gross condensation and re-evaporation terms from thermodynamical considerations that make use of the AGCMs' internal variables. Relevant quantities would include not only central physical ones like temperature, but also highly parameterised quantities such as those associated with moist convection. In particular the complex nature of moist convection entails that the derivation of realistic gross terms is not a trivial task. This has motivated us to implement two different variants of the tracing with simple assumptions regarding the gross terms instead of developing a complex submodel. The two variants reflect the two extremes regarding the question of how large the gross terms C and R are.

In the first case (variant 3-D-s, “strong mixing”) we assume that C and R are very large, meaning that the precipitation mixes rapidly (in case of the discrete layers of the

Atmospheric water vapour tracers

H. F. Goessling and
C. H. Reick

Title Page

Abstract

Introduction

Conclusions

References

Tables

Figures

◀

▶

◀

▶

Back

Close

Full Screen / Esc

Printer-friendly Version

Interactive Discussion



estimate the maximum uncertainty associated with the question of how strongly precipitation mixes on its way towards the surface with the ambient water vapour.

But the main motivation of this work is not to quantify uncertainties associated with full (3-D) moisture tracing, but to investigate the errors that are introduced by vertical integration prior to the tracing, i.e. errors that are associated with 2-D moisture tracing. In Sect. 2 we showed analytically that the 2-D approximation is exact if the “well-mixed” assumption is valid—in this case 2-D and 3-D moisture tracing are identical. Hence one can convert the full 3-D tracing to a scheme that is equivalent to 2-D moisture tracing by imposing artificially well-mixed conditions. This can be achieved by mixing completely the WVTs in each atmospheric column after every model time-step while preserving the vertical profile of the total moisture, leading to the third variant that we implemented:

variant 2-D:
$$q_i(z) = \hat{f}_i \cdot q(z). \quad (22)$$

Please note that it does not matter which of the 3-D variants is taken as a basis for the reduction to the 2-D variant because vertical differences in the WVT tendencies that exist between the two 3-D variants are immediately nullified by the application of Eq. (22).

The fact that the tracing schemes are completely passive, meaning that they do not affect the evolution of the physical model state, allows us to simulate the moisture tracing with different tracing variants on top of binary identical model runs (see the first paragraph of Sect. 3) by using identical initial conditions. We can thus attribute any differences between the results of the tracing variants exclusively to the above described differences between their implementation.

4.2 Technical validation

As described in Sect. 4.1 we do not use ECHAM6’s internal (prognostic) precipitation fluxes for the downward transport of WVTs, but diagnose vertically resolved precipitation fluxes after every time-step. To demonstrate consistency between our diagnosed

Atmospheric water vapour tracers

H. F. Goessling and
C. H. Reick

Title Page

Abstract

Introduction

Conclusions

References

Tables

Figures

◀

▶

◀

▶

Back

Close

Full Screen / Esc

Printer-friendly Version

Interactive Discussion



precipitation rates and the ones computed by ECHAM6, we now compare them with each other.

At the surface, for a proper comparison between the model's internal downward moisture flux and the diagnosed flux it is necessary to add dew to the model's precipitation, because the computation of $C - R$ (Eq. 14) in the lowest atmospheric layer captures not only the net flux between the precipitation and the ambient air, but also the condensation to the surface (though not the evaporation from the surface, because the latter is already treated explicitly). The model's "prognostic precipitation" discussed in the following thus includes dew.

Comparison of the model's prognostic precipitation and the diagnosed precipitation for a single (10-min) time-step reveals that the diagnosed precipitation largely agrees with the prognostic precipitation (Fig. 5, left). For a single time-step the variance explained by the identity function amounts to $\sim 97.2\%$. At some locations the diagnosed precipitation is considerably different from the prognostic precipitation, revealing that the mass of the WVTs and/or the prognostic water are not completely conserved in ECHAM6. The fact that in case of most outliers the dominating process is convective precipitation suggests that a large part of the error is due to the parameterisation of moist convection, though some of the error is probably due to numerical issues (Jöckel et al., 2001). However, averaging precipitation rates over longer periods of time shows that the errors are not systematic (Fig. 5, middle and right): averaged over one month, the diagnosed precipitation is everywhere virtually identical to the prognostic precipitation (variance explained by the identity function: $\sim 99.9\%$). This supports the validity of our implementation.

5 On the validity of the "well-mixed" assumption

In Sect. 2 we showed analytically that the 2-D approximation is exact if the fractions of all WVT species are perfectly well-mixed vertically. Therefore, before comparing results of the different tracing variants 3-D-s, 3-D-w, and 2-D in Sects. 6 and 7, we investigate

Atmospheric water vapour tracers

H. F. Goessling and
C. H. Reick

Title Page

Abstract

Introduction

Conclusions

References

Tables

Figures

◀

▶

◀

▶

Back

Close

Full Screen / Esc

Printer-friendly Version

Interactive Discussion



in this section to what extent the WVT species from different evaporative source regions are actually well-mixed vertically. To this end we analyse results obtained for two sets of source regions using only the 3-D-s moisture tracing variant. Those aspects of the results that we discuss in this section are virtually identical for the 3-D-w variant, which we therefore do not consider here.

The first set of source regions is defined by the model's land-sea mask, meaning that only oceanic and continental moisture are distinguished. In the second set we distinguish four evaporative source regions, of which three are defined by 1000 km × 1000 km-rectangles located on different continents (Table 1, marked by black boxes in Figs. 7, 9, and 11) while the fourth comprises the remainder of the Earth's surface.

To quantify to what extent a WVT species i is well-mixed vertically we define the measure Ψ_i as follows:

$$\Psi_i := 2 \frac{\int_{z^*}^{\infty} \rho q_i dz}{\int_0^{\infty} \rho q_i dz} - 1 \quad (23)$$

where z^* is determined by

$$\frac{\int_{z^*}^{\infty} \rho q dz}{\int_0^{\infty} \rho q dz} = 0.5 \quad (24)$$

which means that half of the total atmospheric moisture resides above z^* and the other half resides below z^* . Obviously, $\Psi_i \in [-1, 1]$, with $\Psi_i = 0$ indicating well-mixed conditions and negative (positive) values indicating higher concentrations in the lower (upper) half of the atmospheric moisture column. Computing Ψ for the moisture of continental origin (Fig. 6) and for the moisture stemming from the three rectangular source regions (Fig. 7) reveals that well-mixed conditions are overall rather scarce.

In Sect. 3 we argued qualitatively that whether the atmosphere is close to well-mixed vertically or not results from the interplay between the generation of vertical inhomogeneities on the one hand and the strength of vertical mixing on the other hand. While

Atmospheric water vapour tracersH. F. Goessling and
C. H. Reick

Title Page

Abstract

Introduction

Conclusions

References

Tables

Figures

◀

▶

◀

▶

Back

Close

Full Screen / Esc

Printer-friendly Version

Interactive Discussion



**Atmospheric water
vapour tracers**H. F. Goessling and
C. H. Reick

Title Page

Abstract

Introduction

Conclusions

References

Tables

Figures

◀

▶

◀

▶

Back

Close

Full Screen / Esc

Printer-friendly Version

Interactive Discussion



vertical inhomogeneities are generated by surface evaporation (Fig. 1, bottom) and by directional shear (Fig. 4), vertical mixing that involves not just the boundary layer but also the free troposphere occurs mainly through the action of deep moist convection (Fig. 2). The fact that well-mixed conditions are relatively rare (Figs. 6 and 7) means that vertical mixing is mostly not strong enough to nullify the generation of inhomogeneities by surface evaporation and directional shear.

The influence of surface evaporation on Ψ is straight forward: while within the respective source region surface evaporation acts to enrich moisture originating from the region in the lower levels of the atmosphere (decreasing Ψ) directly, outside the respective source region surface evaporation acts to enrich moisture originating from the region in the upper levels indirectly by enriching moisture of different origin in the lower levels (increasing Ψ_i). This effect is clearly visible in the patterns of Ψ (Figs. 6 and 7): Ψ_{cont} is mostly negative over land and positive over the ocean, and Ψ_{EEU} , Ψ_{AMA} , and Ψ_{WAF} are mostly negative within the respective regions and positive outside.

Strongly negative values of Ψ inside the source regions only occur where strong moist convection is rare (Fig. 2). Otherwise, a substantial enrichment of local moisture in the lower levels is prevented by vertical mixing. For Ψ_{cont} this is the case for example in large parts of South America in January and in large parts of Eurasia in July. In case of the smaller-scale regions, close to well-mixed conditions inside the region itself occur only in AMA in January due to the vigorous daily mixing by deep convection. At the other extreme are the conditions in EEU in January: here, almost all moisture stemming from the region is concentrated in the lower half of the atmospheric moisture – not only inside the region itself but in large parts of the Northern Hemisphere. This reflects the stable atmospheric stratification that prevails during the northern-hemispheric winter over the northern land and sea-ice areas, effectively suppressing deep convection (Fig. 2).

It is generally an interesting question at which distance from the source regions well-mixed conditions are attained by vertical mixing. Apart from the just mentioned case of EEU in January, negative values of Ψ directly associated with the regions'

surface evaporation are mostly constrained to the close proximity of the respective source regions (Figs. 6 and 7). This means that vertical inhomogeneities generated inside the regions typically do not persist for more than a couple of hundred kilometers until vertical mixing has largely nullified the inhomogeneities. Besides the special case of EEU in January, it seems that also in most of the other cases negative values of Ψ generated inside the source regions are preserved for considerably more than a few hundred kilometers at least in one direction, for example in July to the south of EEU, to the north-west of AMA, and to the east of WAF.

Inspection of the vertical structure of the winds (Fig. 3, top and middle, and Fig. 4) however reveals that it is rather directional shear that is responsible for these negative- Ψ -tails, meaning that they are not simply due to the preservation of the low-level enrichment generated inside the source regions. For example, the tail to the north-west of AMA and the tail to the east of WAF, both in July, are due to a situation where low-level winds advect air masses directly from the respective source region while mid-tropospheric winds blow from a different direction. An analogous situation leads to negative values of Ψ_{EEU} to the south of EEU in July where the westerlies have a significant southward component that is absent in the mid-troposphere. However, in the latter case the “tail” with negative values of Ψ_{EEU} covers a much larger area because the subsiding branch of the Hadley cell south of $\sim 35^\circ$ N is associated with virtual absence of deep convection (Fig. 2), meaning that vertical inhomogeneities are preserved once air masses have entered the subtropics from the north.

Beyond the primary regions of low-level enrichment (negative Ψ) in the vicinity of the respective source regions, Ψ not only attains values around zero, corresponding to well-mixed conditions, but is mostly positive. As mentioned above, this is primarily due to the action of surface evaporation (Fig. 7). However, apart from the narrow transition zones, i.e. where Ψ switches its sign, close to well-mixed conditions also occur in some more distant locations. Most striking is a band of close to well-mixed conditions for all considered source regions (Figs. 6 and 7) near the equator, which is obviously due to

Atmospheric water vapour tracersH. F. Goessling and
C. H. Reick

Title Page

Abstract

Introduction

Conclusions

References

Tables

Figures

◀

▶

◀

▶

Back

Close

Full Screen / Esc

Printer-friendly Version

Interactive Discussion



strong mixing caused by frequently occurring deep convection within the Intertropical Convergence Zone (ITCZ) (Fig. 2).

Well-mixed conditions – and even low-level enrichment – at locations far away from the respective source regions can also be generated by a suitable vertical structure of the winds, where suitable means that the low-level winds advect air from regions containing higher fractions of moisture stemming from the considered source region than the higher-level winds do. This is for example the reason for the negative values of Ψ_{AMA} and Ψ_{WAF} above the tropical Eastern Pacific in January, but also for the negative values of Ψ_{EEU} between Hawaii and California in July (Fig. 7). In the latter case, near-surface winds advect extratropical air masses from the north while mid-tropospheric easterlies advect tropical air masses from the east (Fig. 3, top right and middle right). Because the overall prevailing zonal winds act to mix air masses faster zonally than meridionally, air masses located within the same zonal band as the source region under consideration contain tendentially more moisture stemming from the source region than air masses in other zonal bands. This explains not only why Ψ_{EEU} is strongly negative between Hawaii and California in July, but also why Ψ_{AMA} and Ψ_{WAF} are strongly positive at the same time and place. Moreover, the fact that mixing occurs faster in zonal than in meridional direction also explains why, apart from the direct vicinity of the tropical source regions, the patterns of Ψ_{AMA} and Ψ_{WAF} are generally similar.

Well-mixed conditions for atmospheric moisture of different origin are apparently not the rule. As set out in Sect. 2, this implies that in most places 2-D moisture tracing is necessarily associated with errors. We showed that two types of errors can be distinguished: given the “well-mixed” assumption is not valid, (I) it matters from which level precipitation originates, and (II) the 2-D horizontal advection term (Eq. 11) is not exact. As we show in Sect. 7, both factors are responsible for differences between 2-D and 3-D moisture tracing. But basically only the first of the two factors is responsible for differences between the two 3-D moisture tracing variants 3-D-s and 3-D-w, which is the subject of the following section.

Atmospheric water vapour tracers

H. F. Goessling and
C. H. Reick

Title Page

Abstract

Introduction

Conclusions

References

Tables

Figures

⏪

⏩

◀

▶

Back

Close

Full Screen / Esc

Printer-friendly Version

Interactive Discussion



6 Uncertainties associated with 3-D moisture tracing

Before coming to the main subject of this study, namely the relation between 2-D and 3-D moisture tracing, we first discuss the uncertainties in 3-D tracing arising from the different assumptions on how precipitation mixes with the ambient water vapour. As described in Sect. 4.1 we apply two variants of 3-D moisture tracing: in case of the variant 3-D-s precipitation mixes instantaneously with the ambient water vapour (strong mixing), and in case of the variant 3-D-w no mixing apart from that associated with net condensation/re-evaporation occurs (weak mixing). Since these variants are at the two extremes of the range of possible assumptions, they allow us to estimate the maximum uncertainty associated with the question of how strongly precipitation mixes with the ambient water vapour. In the following we compare tracing results obtained with the two 3-D moisture tracing variants, focussing on the simulated composition of precipitation. We use the same two sets of evaporative source regions considered in the previous section, beginning with the experiments in which a distinction is made between continental and oceanic moisture.

Using the land-sea mask to determine the continents and the ocean as evaporative source regions implies that the results with respect to the composition of precipitation are continental recycling ratios (following Goessling and Reick, 2011, here and in the following we denote continental *precipitation* recycling ratios simply as continental recycling ratios, or R_c). R_c is defined as the (spatially resolved) fraction of precipitation that stems from continental evaporation. Overall, both 3-D moisture tracing variants give very similar patterns of R_c (Fig. 8). In agreement with earlier studies (Numaguti, 1999; Bosilovich et al., 2002; Yoshimura et al., 2004; van der Ent et al., 2010; Goessling and Reick, 2011) we find that R_c increases from continental upwind coasts to downwind coasts with weak seasonality in the tropics and strong seasonality in the extratropics, where the latter is mainly due to the seasonality of evaporation (Fig. 1, bottom). While the highest values of R_c occur in Eastern Eurasia in July with more than 80 %, peak values in the continental tropics are around 60 % throughout the year.

Atmospheric water vapour tracers

H. F. Goessling and
C. H. Reick

Title Page

Abstract

Introduction

Conclusions

References

Tables

Figures

◀

▶

◀

▶

Back

Close

Full Screen / Esc

Printer-friendly Version

Interactive Discussion



**Atmospheric water
vapour tracers**H. F. Goessling and
C. H. Reick

Title Page

Abstract

Introduction

Conclusions

References

Tables

Figures

◀

▶

◀

▶

Back

Close

Full Screen / Esc

Printer-friendly Version

Interactive Discussion



Regarding the computed continental recycling ratios, the most striking difference between 3-D-s and 3-D-w is that 3-D-s almost exclusively gives higher values on the continents and lower values over the ocean (Fig. 8, bottom). To explain this land-ocean contrast one has to recall that, in contrast to the 3-D-w variant, in the 3-D-s variant the precipitation arriving at the surface reflects the composition of the near-surface atmospheric moisture rather than that of the higher-level moisture (compare Sect. 4.1). The land-ocean contrast in the difference pattern can hence be explained by Ψ_{cont} (Fig. 6): on the continents (over the ocean) the fraction of continental (oceanic) moisture in total moisture is larger near the surface than in higher levels. Using a term coined by Lettau et al. (1979), 3-D-s features stronger fast-recycling than 3-D-w, implying that moisture of local origin is overrepresented in precipitation.

There are of course deviations from the correlation between Ψ_{cont} and the differences between 3-D-s and 3-D-w. For example, north of lake Baikal in January 3-D-s gives lower continental recycling ratios albeit Ψ_{cont} is negative. Such discrepancies exist for two reasons: first the definition of Ψ (Eq. 23) implies that Ψ_{cont} only captures differences between the compositions of the lower and the upper half of the atmospheric moisture, although the composition generally also varies within the two halves. Second the average composition of the atmospheric moisture column, although very similar, is not identical between the WVT variants 3-D-s and 3-D-w (not shown) – a secondary consequence of the different implementations. Despite of these two reasons for deviations the patterns are closely correlated, revealing that Ψ_{cont} explains most of the differences in R_c between 3-D-s and 3-D-w.

We now turn to the second set of evaporative source regions (Table 1). Analogously to what we find in the difference patterns of continental recycling ratios, 3-D-s gives higher fractions of locally evaporated moisture in precipitation than 3-D-w within the source regions and lower fractions outside (Fig. 9). The reason is again that locally evaporated water is overrepresented near the surface within the source regions and mostly underrepresented near the surface in the relevant locations outside the source regions (Fig. 7), confirming that the 3-D-s variant features stronger fast-recycling.

At first glance it may surprise that there seem to be no differences between 3-D-s and 3-D-w at some distance from the three source regions (Fig. 9, bottom) although strong vertical inhomogeneities exist globally (Fig. 7). Indeed such differences exist. However, they are noticeable only in relative terms (not shown), not in absolute terms which are shown in Fig. 9, bottom: far away from the relatively small source regions the fraction of moisture stemming from these regions is just very small.

7 Errors introduced by the 2-D approximation

To quantify the errors that are introduced by the 2-D approximation we now compare the results obtained with variant 2-D (which is equivalent to conventional offline 2-D moisture tracing) to the results obtained with the 3-D moisture tracing variants (see Sect. 4.1). In addition to the two sets of evaporative source regions considered in Sects. 5 and 6, here we also consider a third set of source regions that serves to determine the evaporative sources of precipitation in the Western Sahel region – a case investigated by Keys et al. (2012). It has already been hypothesised that the 2-D approximation may lead to large errors in this region (Goessling and Reick, 2011; Dirmeyer, 2011).

First we consider again continental recycling ratios (R_c). Regarding continental-scale features the continental recycling ratios derived with 2-D moisture tracing are not too different from those derived with 3-D moisture tracing (Fig. 10, compare also with Fig. 8). However, the errors introduced by the 2-D approximation are generally larger than the uncertainty associated with 3-D tracing. Further, while results obtained with the two 3-D variants are very similar regarding the shapes of the patterns, the 2-D tracing leads to conspicuously modified shapes. Differences between 2-D and 3-D tracing tend to be largest in the tropics where strong directional shear occurs (Fig. 4). Here, differences in R_c between 2-D and 3-D in some places amount to more than 20 % in either direction.

Atmospheric water vapour tracers

H. F. Goessling and
C. H. Reick

Title Page

Abstract

Introduction

Conclusions

References

Tables

Figures

◀

▶

◀

▶

Back

Close

Full Screen / Esc

Printer-friendly Version

Interactive Discussion



Atmospheric water vapour tracersH. F. Goessling and
C. H. Reick

Title Page

Abstract

Introduction

Conclusions

References

Tables

Figures

◀

▶

◀

▶

Back

Close

Full Screen / Esc

Printer-friendly Version

Interactive Discussion



Compared with 3-D moisture tracing, 2-D moisture tracing gives mostly lower values of R_c on the continents and higher values over the ocean (Fig. 10, middle and bottom). This land-ocean contrast, which is clearer in the extratropics than in the tropics, has the same cause as the land-ocean contrast in the differences between the two 3-D variants (Fig. 8, bottom), namely the fact that moisture of local origin is overrepresented in low levels (Fig. 6). In this respect 3-D-w can be considered an intermediate variant between 3-D-s and 2-D: in the 3-D-s variant the surface precipitation is composed like the near-surface water vapour, in the 3-D-w variant the surface precipitation is composed like the water vapour in those levels where the precipitation is originally formed, and in the 2-D variant the surface precipitation is composed like the vertically averaged atmospheric column.

In Sect. 6 we argued that the 3-D-w variant gives lower continental recycling ratios on the continents than the 3-D-s variant because of weaker fast-recycling. The fact that the 2-D variant, which does not account for fast-recycling at all, gives even lower continental recycling ratios on the continents than the 3-D-w variant suggests that the 3-D-w variant still features some fast-recycling. As an aside, this implies that, at least in ECHAM6, precipitation on average forms at those relatively low levels where there is still a noticeable enrichment of locally evaporated moisture.

For the extratropics the difference patterns of R_c (Fig. 10, middle and bottom) and Ψ_{cont} (Fig. 6) suggest that the neglect of fast-recycling is the main reason for errors associated with the 2-D approximation. In the tropics, however, another factor comes into play. The spatial patterns of R_c derived with 2-D and 3-D moisture tracing exhibit a characteristic structural difference: the continental recycling ratios derived with 2-D tracing tend to have steeper gradients, most strikingly to the west of both Africa and South America in the vicinity of the equator. Also, while in the extratropics errors introduced by the 2-D approximation are rather shape preserving, the errors in the tropics are associated with changes in the shape of the patterns of R_c . The reason for these structural differences (the steeper gradients and the modified pattern shapes obtained with 2-D tracing) is that in the tropics directional shear (Fig. 4) causes basically horizontal

dispersion of atmospheric moisture components, resulting in smoothed horizontal gradients. This effect is missing in the vertically integrative 2-D approach. It is hence in these tropical regions where the largest differences, not only in magnitude but also in shape, between continental recycling ratios obtained with 2-D and 3-D moisture tracing occur.

The already described difference between the tropics and the extratropics is also evident in the results for the three smaller evaporative source regions (Fig. 11, middle and bottom). Within EEU the 2-D approximation substantially underestimates the fraction of local moisture in precipitation, and outside EEU the fraction of moisture from EEU in precipitation is overestimated. The main explanation for this is, again, the neglect of fast-recycling. For the tropical regions AMA and WAF there is apparently also an element of this, causing mostly an underestimation of recycling within the source regions and an overestimation outside. However, the shape of the resulting patterns is considerably altered by the 2-D approximation only in the tropics. This is most obvious in July: while 3-D moisture tracing reveals that moisture evaporated from WAF is preferentially advected northeastward (Fig. 9, top right and middle right), the results of the 2-D approximation suggest that the moisture is mainly advected westward (Fig. 11, top right). For moisture evaporated from AMA in July, 3-D moisture tracing gives highest fractions in precipitation along the western boundary of the source region, whereas the 2-D approximation gives peak values in the southwestern corner. An even more salient difference in this case is that the 2-D approximation diagnoses that substantial amounts of moisture stemming from AMA precipitate over the tropical Eastern Pacific – a feature that the full tracing reveals as an artefact.

These errors in the tropics are obviously due to the layered structure of the atmosphere. In AMA in July, the monsoonal layer below ~ 750 hPa carries air masses north-eastward while the African easterly jet above ~ 750 hPa blows westward (Fig. 3, top right and middle right). Due to the high wind speeds, the horizontal moisture flux associated with the African easterly jet outweighs the flux associated with the moister but slower moving monsoonal layer, explaining why the 2-D variant diagnoses a westward

Atmospheric water vapour tracersH. F. Goessling and
C. H. Reick

Title Page

Abstract

Introduction

Conclusions

References

Tables

Figures

◀

▶

◀

▶

Back

Close

Full Screen / Esc

Printer-friendly Version

Interactive Discussion



advection of moisture (Fig. 3, bottom right). This leads to erroneous results because most of the moisture stemming from WAF is concentrated in the northwestward flowing monsoonal layer (Fig. 7, bottom right). An analogous explanation can be given for the differences seen in AMA in July described above, where the prevailing easterlies have a northward component near the surface but a southward component in the mid-troposphere (Fig. 3, top right and middle right), combined with considerably non-zero values of Ψ_{AMA} (Fig. 7, middle right).

The meteorological conditions in these regions are different in January. At this time of the year WAF is subject to subtropical large-scale subsidence, the ITCZ being located further to the south (Fig. 1, top left). Because of the associated absence of precipitation this region is not very interesting in the context of our study at that time of the year. By contrast, AMA, located south of the equator, receives considerably more precipitation in January than in July. The higher frequency of strong moist convection in January (Fig. 2) is associated with stronger vertical mixing. This in combination with a relatively low degree of directional shear (Fig. 4) acts to prevent significant enrichment of local moisture near the surface (Fig. 7, middle left). Consequently, in AMA in January the 2-D approximation gives reasonable results, the only deficit seeming to be the neglect of a moderate degree of fast-recycling (Fig. 11, left).

As discussed above, the transport of moisture evaporated from WAF in July can be determined only poorly using the 2-D approximation. The reason for this is that, given the strong generation of vertical inhomogeneities by surface evaporation and by directional shear, the counteracting degree of vertical mixing does not suffice to establish well-mixed conditions. This already indicates that, likewise, the evaporative source regions for precipitation in the nearby located Western Sahel can probably not be diagnosed adequately using the 2-D approximation.

Keys et al. (2012) diagnosed the evaporative sources for precipitation in the Western Sahel (and other regions) applying 2-D moisture tracing to ERA-Interim reanalysis data (Dee et al., 2011). In the following we investigate how much error in this specific case must be expected to arise from the use of the 2-D approximation. To this end we apply

Atmospheric water vapour tracersH. F. Goessling and
C. H. Reick

Title Page

Abstract

Introduction

Conclusions

References

Tables

Figures

◀

▶

◀

▶

Back

Close

Full Screen / Esc

Printer-friendly Version

Interactive Discussion



all three moisture tracing variants to a third set of evaporative source regions comprising Africa (AFR), those regions located to the southwest of Africa (SW), those regions located to the southeast of Africa (SE), and the remainder, i.e. those regions located to the north of Africa (N) (Fig. 12). When we refer to the Western Sahel, we mean the rectangular region ranging from 8.4° W to 17.8° E and from 11.2° N to 16.8° N (see the black rectangles in Figs. 12 and 14), which is approximately the same region as the one investigated by Keys et al. (2012).

The contributions to Western Sahelian precipitation from AFR and SE are reasonably well reproduced by the 2-D approximation, but the contributions from N and SW are not (Table 2, Figs. 13 and 14); while the well-agreeing 3-D variants reveal that approximately equal amounts stem from N and SW, the 2-D variant almost completely misses the contribution from SW, compensated by an increased contribution from N. The reason for this deficit is, as already discussed for the moisture stemming from WAF, the layered structure of the atmosphere: the low-level monsoonal layer advects air masses from the southwest while the African Easterly Jet above advects air masses from the northeast (Fig. 3), whereby vertical mixing is not strong enough to maintain well-mixed conditions.

In accordance with the results from our 2-D variant, Keys et al. (2012) found much less moisture stemming from the tropical Atlantic than from the mediterranean and the adjacent regions. Our results obtained with a resolved vertical dimension however indicate that the contributions are approximately equal. It thus seems that the precipitations of the Western Sahel as determined by Keys et al. (2012) (see Fig. 3 therein) is strongly biased towards the northeast.

8 Discussion

In the following we first discuss potential model deficits and compare important atmospheric characteristics as simulated with ECHAM6 to ERA-Interim data (Dee et al., 2011). Thereafter follows a comment on a (further) methodological difference between

Atmospheric water vapour tracers

H. F. Goessling and
C. H. Reick

Title Page

Abstract

Introduction

Conclusions

References

Tables

Figures



Back

Close

Full Screen / Esc

Printer-friendly Version

Interactive Discussion



Keys et al. (2012) and our study. We then discuss further aspects that are associated with the distinction between net and gross rates of evaporation and condensation, leading finally to the question of what should be the guiding principle for the development of a “best” way to trace moisture in the atmosphere.

Of course ECHAM6’s climate contains unavoidable biases, and the usage of climatological SSTs in this study adds to these. One may therefore wonder if our results can be transferred to the real world. First, our theoretical considerations are of course not affected. Second, we relate the simulated differences between 2-D and 3-D moisture tracing to atmospheric characteristics that can likewise be evaluated for other atmospheric data sets like reanalysis data. This way potential differences between our findings and the real world (approximated by reanalysis data) can be assessed. In fact, the key atmospheric characteristics seem to be, at least qualitatively, reasonably well reproduced by ECHAM6, as the following comparison with ERA-Interim data (Dee et al., 2011) shows.

One strength of AGCMs clearly lies in their ability to reproduce large-scale circulation patterns relatively well, because these are to a large extent determined by the physically well-founded primitive equations at resolved scales, and to a lesser extent by uncertain parameterisations such as those needed for moist convective processes. The comparison of the horizontal winds as simulated by ECHAM6 (Fig. 3, top and middle) with ERA-Interim data (Fig. 15) supports this notion. Features of the vertical wind structure that we referred to in the previous sections are confirmed to exist also in the real world, including for example the layered structure in tropical Western Africa.

Somewhat less well reproduced by ECHAM6, at least when driven with climatological SSTs as in this study, appears to be the frequency of strong moist convection (Fig. 16, compare Fig. 2). While the overall spatial pattern is clearly captured, ECHAM6 tends to underestimate the frequency of days with convective precipitation exceeding 10 % of the atmosphere’s vertically integrated moisture content. This suggests that ECHAM6 tends to underestimate the degree of vertical mixing in the free troposphere, though this potential deficit should be of quantitative rather than qualitative nature. Regarding the

Atmospheric water vapour tracers

H. F. Goessling and
C. H. Reick

Title Page

Abstract

Introduction

Conclusions

References

Tables

Figures

⏪

⏩

◀

▶

Back

Close

Full Screen / Esc

Printer-friendly Version

Interactive Discussion



extensively discussed region of tropical Western Africa, it seems worth to mention that in this region ECHAM6 apparently reproduces the frequency of strong moist convection reasonably well.

It should be mentioned that Keys et al. (2012) applied their diagnostic 2-D moisture tracing scheme not forward in time, but backward. This allowed them to determine the evaporative source regions for precipitation in the Western Sahel (and in other regions) at grid-point spatial resolution, whereas we, keeping to forward tracing, distinguished only four large predetermined source regions. However, the differences between 2-D and 3-D tracing should not depend on the temporal direction in which the tracing is carried out.

In Sect. 6 we pointed out that 3-D, i.e. “full”, moisture tracing itself bears some uncertainties, even if the underlying atmospheric model is assumed to be perfect. These uncertainties arise from the fact that the evolution of the atmosphere’s physical state does not depend on gross but only on net rates of condensation and re-evaporation, i.e. their difference $C - R$, making it unnecessary to work with gross rates in atmospheric models. However, a precise tracing of moisture requires knowledge of the gross rates, because these are needed to determine to what extent precipitation mixes with the ambient water vapour. The two 3-D moisture tracing variants we applied are at the two extremes of the possible range of assumptions. This means that it could well be possible to narrow down the uncertainty associated with this issue by incorporating existing knowledge about the degree of mixing between precipitation and the ambient water vapour. Such knowledge could be derived from measurements of stable water isotopes, from targeted smaller-scale modelling studies, or even from simple thermodynamical considerations. It could also make sense to distinguish different precipitation generating mechanisms, foremost convective and large-scale processes, as the following considerations suggest.

During deep convective events precipitation occurs in the relatively narrow convective updrafts only. The precipitation exchanges water molecules only with the ambient water vapour inside the updrafts and, accounting for entrainment and detrainment, with

Atmospheric water vapour tracers

H. F. Goessling and
C. H. Reick

Title Page

Abstract

Introduction

Conclusions

References

Tables

Figures



Back

Close

Full Screen / Esc

Printer-friendly Version

Interactive Discussion



Atmospheric water vapour tracersH. F. Goessling and
C. H. Reick

Title Page

Abstract

Introduction

Conclusions

References

Tables

Figures

◀

▶

◀

▶

Back

Close

Full Screen / Esc

Printer-friendly Version

Interactive Discussion



the immediate surroundings of the updrafts. This means that equilibration with respect to composition between precipitation and ambient water vapour happens only within the updrafts, while the air in the much larger downdrafts is not in contact with the precipitation. This suggests that the composition of the precipitation arriving at the surface is to a relatively large degree determined by the composition of the upper-level atmospheric moisture from which the precipitation originally formed.

By contrast, stratiform (large-scale) precipitation is characterised by rather uniform horizontal conditions, meaning that precipitation exchanges water molecules with the large water vapour reservoir of all the air. This suggests that in stratiform situations the composition of the precipitation arriving at the surface is not so much determined by the composition of the upper-level atmospheric moisture from which the precipitation originally formed, but rather resembles the composition of the lower-level atmospheric moisture. The latter seems particularly reasonable if the rain drops are relatively small, which is more common for stratiform precipitation than for convective precipitation. These differences between stratiform and convective precipitation suggest that the 3-D-s variant may rather resemble stratiform precipitation, whereas the 3-D-w variant may rather resemble convective precipitation. However, we leave such prospects regarding the optimisation of 3-D moisture tracing open for future research.

A final thought shall carry the issue associated with the distinction of gross and net rates of condensation and re-evaporation even further. We point out that the lack of necessity to determine the gross rates within AGCMs curtails the possibility to perform “perfect” 3-D moisture tracing with passive water vapour tracers, where “perfect” means that the origin and fate of water is correctly determined at the molecular level. Instead, subtle degrees of freedom exist in the system that can only be accounted for with additional assumptions. Strictly speaking, this problem exists not only at the interfaces between condensed and gaseous water compartments in the atmosphere, but also at the Earth’s surface. Consider for example an air mass that is saturated with respect to the ocean’s surface temperature residing over the ocean. In this case net

evaporation/condensation is zero, yet gross evaporation and gross condensation take place and cause an exchange of water molecules.

A “perfect” moisture tracing would have to account for these additional gross exchange fluxes as well. This admittedly peculiar conclusion brings to mind the question what the benefit of a truly perfect moisture tracing would be, apart from the mere satisfaction of intellectual curiosity. We think that the ultimate purpose of moisture tracing is to learn something about causality within the atmospheric branch of the hydrological cycle, to help finding answers to questions of the kind “How does precipitation in B depend on evaporation in A?”. This ultimate purpose of moisture tracing should be the guiding principle for the development of a “best” way to trace moisture in the atmosphere. But is a moisture tracing that is perfect on the molecular level also the best way to determine causalities? Or is it possible that a tracing procedure that omits gross rates and accounts only for net rates is more suitable to determine causal connections between evaporation and precipitation? This issue seems to have escaped the attention of the scientific community and, to our opinion, deserves future exploration.

9 Summary and conclusions

The primary focus of this study is the assessment of errors that are introduced by the application of 2-D moisture tracing as opposed to the “exact” method of 3-D moisture tracing. To this end we analysed the theoretical basis of the 2-D approximation – the “well-mixed” assumption – and implemented both 3-D and 2-D moisture tracing into an AGCM, which allowed us to make a direct quantitative comparison. Moreover, we implemented and evaluated two different 3-D moisture tracing variants to account for the indeterminate degree of mixing that takes place between falling precipitation and the ambient water vapour.

We showed analytically that 2-D moisture tracing is exact if the “well-mixed” assumption holds; in this case neither horizontal advection nor the precipitation process are associated with errors due to the 2-D approximation. Accordingly, the accuracy of the

Atmospheric water vapour tracers

H. F. Goessling and
C. H. Reick

Title Page

Abstract

Introduction

Conclusions

References

Tables

Figures

◀

▶

◀

▶

Back

Close

Full Screen / Esc

Printer-friendly Version

Interactive Discussion



**Atmospheric water
vapour tracers**H. F. Goessling and
C. H. Reick

Title Page

Abstract

Introduction

Conclusions

References

Tables

Figures

◀

▶

◀

▶

Back

Close

Full Screen / Esc

Printer-friendly Version

Interactive Discussion



2-D approximation is highest where meteorological conditions are favourable of well-mixed conditions, and lowest where strong vertical inhomogeneities are present. We demonstrated that key atmospheric characteristics in this context are (I) the presence of directional shear, which generates vertical inhomogeneities, and (II) the frequency of deep convection, which acts to mix the atmosphere vertically. Overall, well-mixed conditions are seldom met and, hence, the 2-D approximation is mostly associated with noticeable errors.

One can discern two kinds of errors introduced by the 2-D approximation, namely (I) the omission of fast-recycling, which leads to an underestimation of local moisture in precipitation but does not greatly affect the spatial structure of the resulting patterns, and (II) the omission of layered horizontal advection, which can have a strong impact on the spatial structure of the resulting patterns and, hence, appears to be the more serious deficit of 2-D moisture tracing. We find a different degree of fast-recycling also to be the main reason for differences between the two 3-D moisture tracing variants, whereas layered advection is not a factor there. As a consequence, the (pattern distorting) errors introduced by the 2-D approximation are generally larger than the (pattern conserving) uncertainties associated with 3-D moisture tracing.

While the presence of fast-recycling is geographically not much constrained, strongly layered advection is a distinctive feature of the tropics with its thermally direct circulations; the latter are suppressed in the extratropics where the Coriolis force gives rise to a certain vertical rigidity of the atmosphere. There are, of course, also in the tropics situations where the winds are only moderately sheared vertically and, if in combination with frequent vertical mixing, the errors resulting from the 2-D approximation are as moderate as they tend to be in the extratropics. This is for example the case for the Amazon region in January. The rule however is that the 2-D approximation is less appropriate in the tropics, in particular where strong directional shear combines with a low frequency of moist convective mixing.

An example for such a region is tropical Western Africa (including the Western Sahel), where in particular during the monsoon season (northern summer) the

atmosphere's vertical structure is strongly layered and moist convective mixing does by far not suffice to maintain well-mixed conditions. Here, 2-D moisture tracing strongly underestimates the amount of moisture originating from the tropical Atlantic that, in reality, is transported in the low-level monsoonal layer far into the African continent.

5 Compensatingly, 2-D moisture tracing overestimates the contribution to Western Sahelian precipitation originating from beyond the Sahara.

We think that, due to its simplicity and straightforward applicability to different kinds of data, 2-D moisture tracing is a useful approximation despite the errors that are introduced by the vertical integration. However, its application should largely be constrained
10 to the extratropics, or, if applied to tropical regions, it should be made sure that the atmospheric conditions at the place and time are such that errors associated with the 2-D approximation can be assumed to be small. Our study can be used as a basis for deciding when and where 2-D moisture tracing can be considered a useful approximation.

15 *Acknowledgements.* We thank Veronika Gayler and Reiner Schnur for helping us implement WVTs into ECHAM6. Sebastian Rast also supported us with the implementation and in addition gave valuable comments on the manuscript, for which we are very grateful. The simulations were carried out on the supercomputing system of the German Climate Computing Center (DKRZ) in Hamburg. Most of the figures were generated with the NCAR Command
20 Language (<http://dx.doi.org/10.5065/D6WD3XH5>). The ERA-Interim data (Dee et al., 2011) were provided by the European Centre for Medium-Range Weather Forecasts via the World Data Center for Climate in Hamburg.

The service charges for this open access publication
25 have been covered by the Max Planck Society.

Atmospheric water vapour tracers

H. F. Goessling and
C. H. Reick

Title Page

Abstract

Introduction

Conclusions

References

Tables

Figures



Back

Close

Full Screen / Esc

Printer-friendly Version

Interactive Discussion



References

- Bosilovich, M. G.: On the vertical distribution of local and remote sources of water for precipitation, *Meteorol. Atmos. Phys.*, 80, 31–41, 2002. 30121, 30123
- Bosilovich, M. G. and Schubert, S. D.: Water vapor tracers as diagnostics of the regional hydrologic cycle, *J. Hydrometeorol.*, 3, 149–165, 2002. 30121
- 5 Bosilovich, M. G., Sud, Y., Schubert, S. D., and Walker, G. K.: GEWEX CSE sources of precipitation using GCM water vapor tracers, *Global Energy and Water Cycle Experiment NEWS*, 3, 6–7, 2002. 30121, 30143
- Brubaker, K. L., Entekhabi, D., and Eagleson, P. S.: Estimation of continental precipitation recycling, *J. Climate*, 6, 1077–1089, 1993. 30123
- 10 Budyko, M. I.: *Climate and Life*, Int. Geophys. Ser., Academic Press, New York and London, 18, 1974. 30123
- Burde, G. I.: Bulk recycling models with incomplete vertical mixing. Part I: Conceptual framework and models, *J. Climate*, 19, 1461–1472, 2006. 30123
- 15 Dansgaard, W.: Stable isotopes in precipitation, *Tellus*, 16, 436–468, 1964. 30121
- Dee, D., Uppala, S., Simmons, A., Berrisford, P., Poli, P., Kobayashi, S., Andrae, U., Balmaseda, M., Balsamo, G., Bauer, P., Bechtold, P., Beljaars, A. C. M., van de Berg, L., Bidlot, J., Bormann, N., Delsol, C., Dragani, R., Fuentes, M., Geer, A. J., Haimberger, L., Healy, S. B., Hersbach, H., Hólm, E. V., Isaksen, I., Kållberg, P., Köhler, M., Matricardi, M., McNally, A. P., Monge-Sanz, B. M., Morcrette, J.-J., Park, B.-K., Peubey, C., de Rosnay, P., Tavolato, C., Thépaut, J.-N., and Vitart, F.: The ERA-Interim reanalysis: configuration and performance of the data assimilation system, *Q. J. Roy. Meteor. Soc.*, 137, 553–597, 2011. 30148, 30149, 30150, 30155, 30175, 30176
- 20 Dirmeyer, P.: Interactive comment on “Analyzing precipitation sheds to understand the vulnerability of rainfall dependent regions” by Keys et al., *Biogeosciences Discuss.*, 8, C4544–C4546, 2011. 30145
- Dirmeyer, P. and Brubaker, K.: Contrasting evaporative moisture sources during the drought of 1988 and the flood of 1993, *J. Geophys. Res.*, 104, p. 19383 doi:10.1029/1999JD900222, 1999. 30122
- 25 Eltahir, E. A. B. and Bras, R. L.: Precipitation recycling in the Amazon basin, *Q. J. Roy. Meteor. Soc.*, 120, 861–880, 1994. 30123
- 30

Atmospheric water vapour tracers

H. F. Goessling and
C. H. Reick

Title Page

Abstract

Introduction

Conclusions

References

Tables

Figures

◀

▶

◀

▶

Back

Close

Full Screen / Esc

Printer-friendly Version

Interactive Discussion



Atmospheric water vapour tracers

H. F. Goessling and
C. H. Reick

Title Page

Abstract

Introduction

Conclusions

References

Tables

Figures

◀

▶

◀

▶

Back

Close

Full Screen / Esc

Printer-friendly Version

Interactive Discussion



- Fitzmaurice, J. A.: A critical analysis of bulk precipitation recycling models, Ph. D. thesis, Massachusetts Institute of Technology, 2007. 30123
- Garratt, J.: The Atmospheric Boundary Layer, Cambridge University Press, Cambridge, 1992. 30132
- 5 Goessling, H. F. and Reick, C. H.: What do moisture recycling estimates tell us? Exploring the extreme case of non-evaporating continents, *Hydrol. Earth Syst. Sci.*, 15, 3217–3235, doi:10.5194/hess-15-3217-2011, 2011. 30121, 30122, 30123, 30143, 30145
- Jöckel, P., von Kuhlmann, R., Lawrence, M., Steil, B., Brenninkmeijer, C., Crutzen, P., Rasch, P., and Eaton, B.: On a fundamental problem in implementing flux-form advection schemes for tracer transport in 3-dimensional general circulation and chemistry transport models, *Q. J. Roy. Meteor. Soc.*, 127, 1035–1052, 2001. 30132, 30138
- 10 Jousaume, S., Sadourny, R., and Vignal, C.: Origin of precipitating water in a numerical simulation of July climate, *Ocean-Air Interact.*, 1, 43–56, 1986. 30121
- Keys, P. W., van der Ent, R. J., Gordon, L. J., Hoff, H., Nikoli, R., and Savenije, H. H. G.: Analyzing precipitation sheds to understand the vulnerability of rainfall dependent regions, *Biogeosciences*, 9, 733–746, doi:10.5194/bg-9-733-2012, 2012. 30122, 30145, 30148, 30149, 30150, 30151
- 15 Koster, R., Jouzel, J., Suozzo, R., Russell, G., Broecker, W., Rind, D., and Eagleson, P.: Global sources of local precipitation as determined by the Nasa/Giss GCM, *Geophys. Res. Lett.*, 13, 121–124, 1986. 30121
- 20 Lettau, H., Lettau, K., and Molion, L. C. B.: Amazonia's hydrologic cycle and the role of atmospheric recycling in assessing deforestation effects, *Mon. Weather Rev.*, 107, 227–238, 1979. 30144
- Lin, S.-J. and Rood, R.: Multidimensional flux-form semi-Lagrangian transport schemes, *Mon. Weather Rev.*, 124, 2046–2070, 1996. 30132
- 25 Nordeng, T.: Extended versions of the convection parametrization scheme at ECMWF and their impact upon the mean climate and transient activity of the model in the tropics, Tech. rep., Research Department Technical Memorandum, ECMWF, Reading, UK, 1994. 30132
- Numaguti, A.: Origin and recycling processes of precipitating water over the Eurasian continent: experiments using an atmospheric general circulation model, *J. Geophys. Res.*, 104, 1957–1972, 1999. 30143
- 30 Roeckner, E., Baeuml, G., Bonaventura, L., Brokopf, R., Esch, M., Giorgetta, M., Hagemann, S., Kirchner, I., Kornblueh, L., Manzini, E., Rhodin, A., Schlese, U., Schulweida, U., and Tomp-

Atmospheric water vapour tracers

H. F. Goessling and
C. H. Reick

Title Page

Abstract

Introduction

Conclusions

References

Tables

Figures

◀

▶

◀

▶

Back

Close

Full Screen / Esc

Printer-friendly Version

Interactive Discussion



kins, A.: The atmospheric general circulation model ECHAM5. Part I: Model description, Tech. Rep. 349, Max Planck Institute for Meteorology, Hamburg, Germany, 2003. 30128, 30132

Salati, E., Dall'Olio, A., Matsui, E., and Gat, J. R.: Recycling of water in the Amazon basin: an isotopic study, *Water Resour. Res.*, 15, 1250–1258, 1979. 30121

Silberberg, M., Duran, R., Haas, C., and Norman, A.: Chemistry: the Molecular Nature of Matter and Change, Mosby, St. Louis, 1996. 30133

Sodemann, H., Wernli, H., and Schwierz, C.: Sources of water vapour contributing to the Elbe flood in August 2002 – a tagging study in a mesoscale model, *Q. J. Roy. Meteor. Soc.*, 135, 205–223, 2009. 30121

Stohl, A. and James, P.: A Lagrangian analysis of the atmospheric branch of the global water cycle. Part I: Method description, validation, and demonstration for the August 2002 flooding in Central Europe, *J. Hydrometeorol.*, 5, 656–678, 2004. 30122

Tiedtke, M.: A comprehensive mass flux scheme for cumulus parameterization in large-scale models, *Mon. Weather Rev.*, 117, 1779–1800, 1989. 30132

van der Ent, R. J. and Savenije, H. H. G.: Length and time scales of atmospheric moisture recycling, *Atmos. Chem. Phys.*, 11, 1853–1863, doi:10.5194/acp-11-1853-2011, 2011. 30122

van der Ent, R. J., Savenije, H. H. G., Schaefli, B., and Steele-Dunne, S. C.: Origin and fate of atmospheric moisture over continents, *Water Resour. Res.*, 46, W09525, doi:10.1029/2010WR009127, 2010. 30121, 30122, 30143

Yoshimura, K., Oki, T., Ohte, N., and Kanae, S.: Colored moisture analysis estimates of variations in 1998 Asian monsoon water sources, *J. Meteorol. Soc. Jpn.*, 82, 1315–1329, 2004. 30122, 30143

Atmospheric water vapour tracers

H. F. Goessling and
C. H. Reick

Title Page

Abstract

Introduction

Conclusions

References

Tables

Figures

◀

▶

◀

▶

Back

Close

Full Screen / Esc

Printer-friendly Version

Interactive Discussion



Table 1. Locations of the rectangular source regions.

Name	abbrev.	meridional range (° N)	zonal range (° E)
Eastern Europe	EEU	50.4–59.7	30.9–47.8
Amazonia	AMA	–9.3–0.0	295.3–304.7
Western Africa	WAF	7.5–16.8	0.0–9.3

**Atmospheric water
vapour tracers**H. F. Goessling and
C. H. Reick

Title Page

Abstract

Introduction

Conclusions

References

Tables

Figures

◀

▶

◀

▶

Back

Close

Full Screen / Esc

Printer-friendly Version

Interactive Discussion



Table 2. Contribution to annual precipitation in the Western Sahel from the four evaporative source regions N, SW, SE, and AFR (compare Fig. 12) as determined by the moisture tracing variants 3-D-s, 3-D-w, and 2-D.

Source region	3-D-s	3-D-w	2-D
N	22 %	22 %	40 %
SW	24 %	26 %	4 %
SE	14 %	14 %	16 %
AFR	40 %	38 %	40 %

**Atmospheric water
vapour tracers**H. F. Goessling and
C. H. Reick

Title Page

Abstract

Introduction

Conclusions

References

Tables

Figures

◀

▶

◀

▶

Back

Close

Full Screen / Esc

Printer-friendly Version

Interactive Discussion

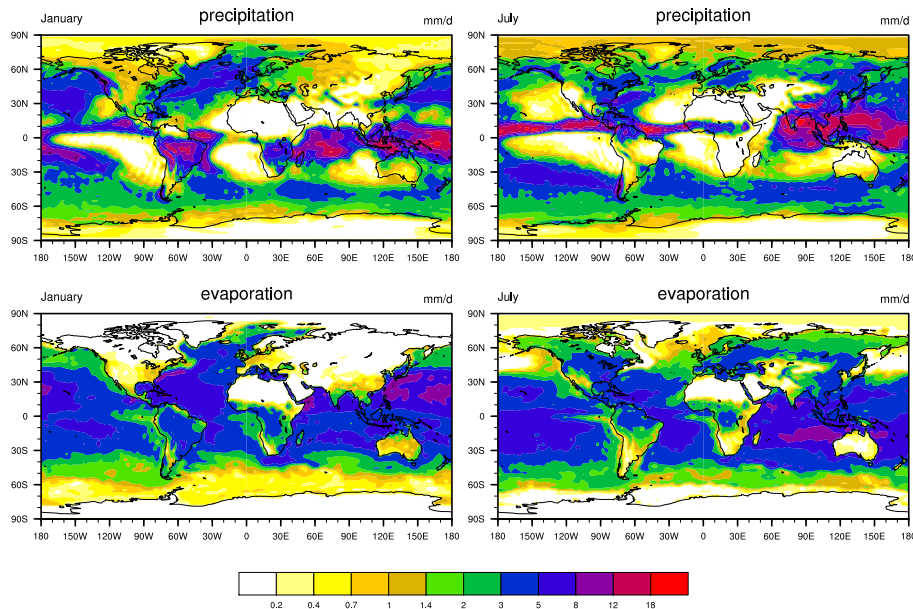


Fig. 1. Simulated precipitation (top, mm d^{-1}) and evaporation (bottom, mm d^{-1}) for January (left) and July (right).

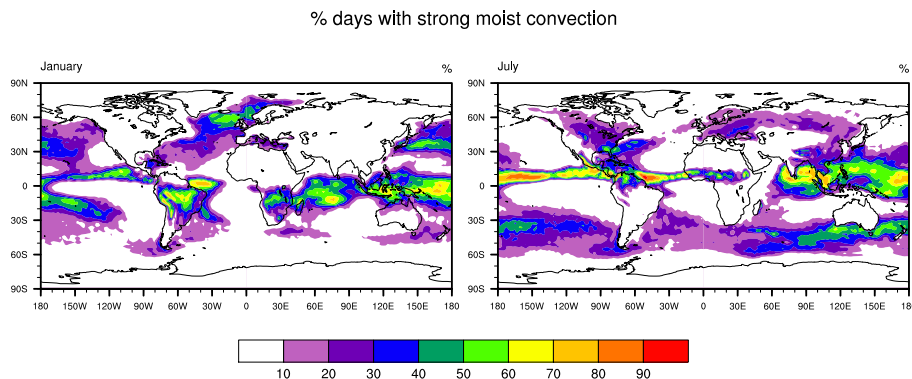
Atmospheric water vapour tracersH. F. Goessling and
C. H. Reick

Fig. 2. Fraction of days with strong moist convection for January (left) and July (right), where we consider events as strong if the generated daily amount of convective precipitation exceeds 10% of the total column water content.

[Title Page](#)[Abstract](#)[Introduction](#)[Conclusions](#)[References](#)[Tables](#)[Figures](#)[◀](#)[▶](#)[◀](#)[▶](#)[Back](#)[Close](#)[Full Screen / Esc](#)[Printer-friendly Version](#)[Interactive Discussion](#)

Atmospheric water
vapour tracersH. F. Goessling and
C. H. Reick

Title Page

Abstract

Introduction

Conclusions

References

Tables

Figures

◀

▶

◀

▶

Back

Close

Full Screen / Esc

Printer-friendly Version

Interactive Discussion

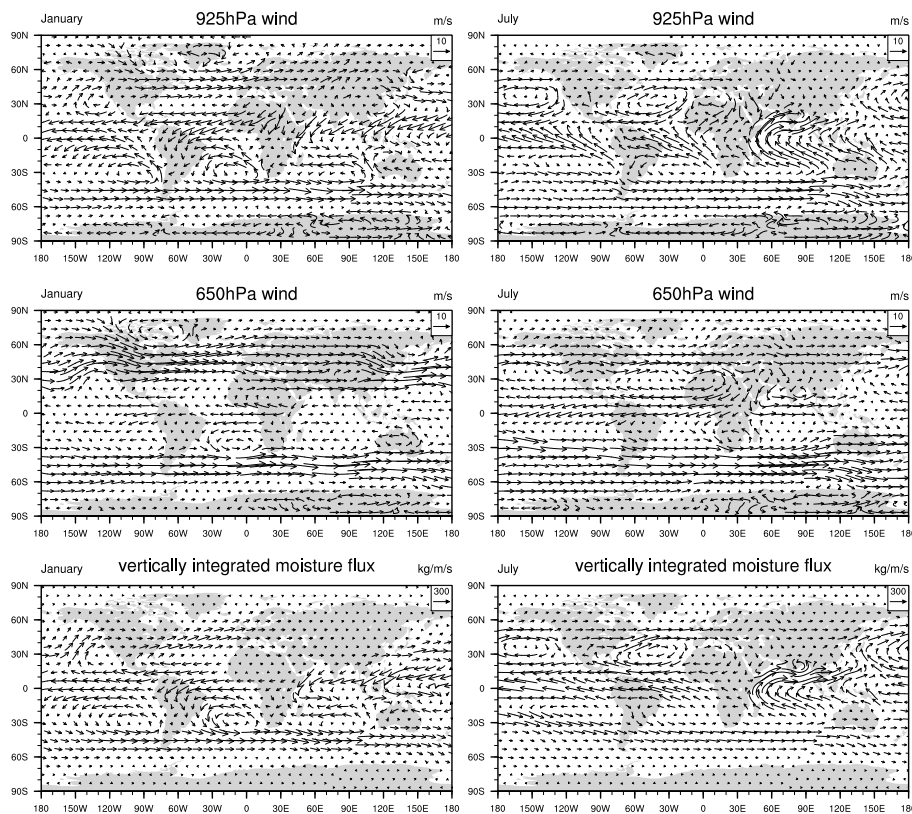


Fig. 3. Horizontal winds at 925 hPa (top, m s^{-1}) and 650 hPa (middle, m s^{-1}), and vertically integrated moisture flux (bottom, $\text{kg m}^{-1} \text{s}^{-1}$) for January (left) and July (right).

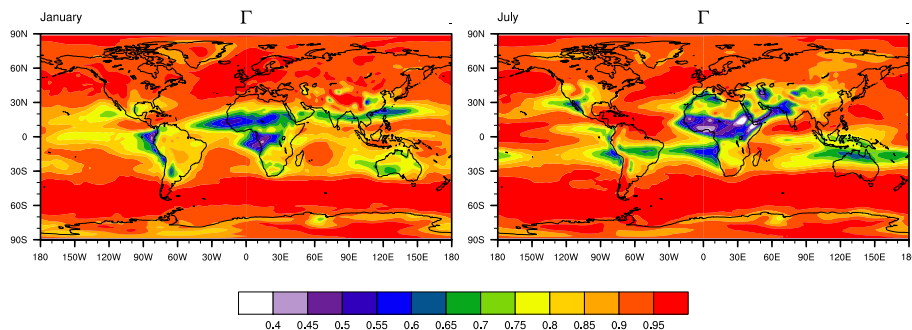
Atmospheric water vapour tracersH. F. Goessling and
C. H. Reick

Fig. 4. Directional shear as measured by Γ (Eq. 12) for January (left) and July (right). Please note that the numerator and the denominator in Eq. (12) are averaged separately over time.

Title Page

Abstract

Introduction

Conclusions

References

Tables

Figures

◀

▶

◀

▶

Back

Close

Full Screen / Esc

Printer-friendly Version

Interactive Discussion



Atmospheric water vapour tracers

H. F. Goessling and
C. H. Reick

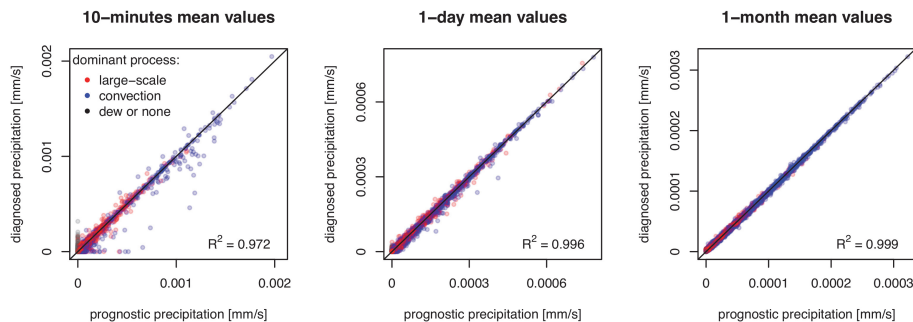


Fig. 5. Prognostic precipitation (including dew) versus diagnosed precipitation (see Eq. 15) at the surface. Left: values of a single (i.e. 10 min) time-step. Middle: values averaged over one day. Right: mean values averaged over one month. Each of the 18 432 points represents one grid cell of the AGCM. The black line denotes identity. The colours indicate which process contributes most to the prognostic precipitation, either stratiform (large-scale) precipitation (red), convective precipitation (blue), or dew or none (black). R^2 is the fraction of variance explained by the identity function.

[Title Page](#)
[Abstract](#)
[Introduction](#)
[Conclusions](#)
[References](#)
[Tables](#)
[Figures](#)
[◀](#)
[▶](#)
[◀](#)
[▶](#)
[Back](#)
[Close](#)
[Full Screen / Esc](#)
[Printer-friendly Version](#)
[Interactive Discussion](#)

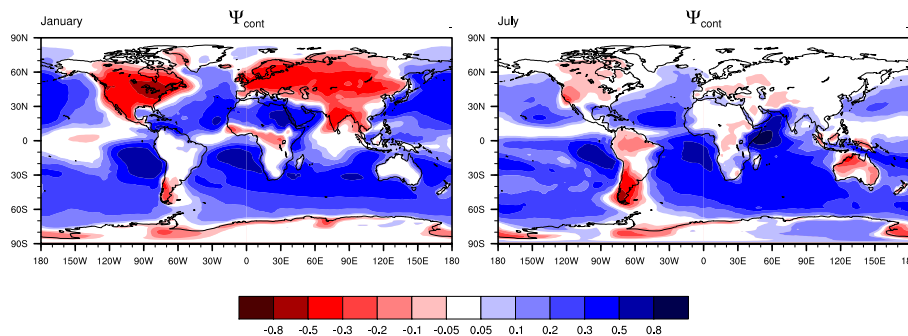

Atmospheric water vapour tracersH. F. Goessling and
C. H. Reick

Fig. 6. The degree to which moisture of continental origin is overrepresented in the upper half (positive values) or the lower half (negative values) of the atmospheric moisture column (Ψ_{cont} , Eq. (23), for January (left) and July (right). The results shown here are calculated for the 3-D-s variant; those for the 3-D-w variant are very similar (not shown).

[Title Page](#)[Abstract](#)[Introduction](#)[Conclusions](#)[References](#)[Tables](#)[Figures](#)[◀](#)[▶](#)[◀](#)[▶](#)[Back](#)[Close](#)[Full Screen / Esc](#)[Printer-friendly Version](#)[Interactive Discussion](#)

Atmospheric water vapour tracers

H. F. Goessling and
C. H. Reick

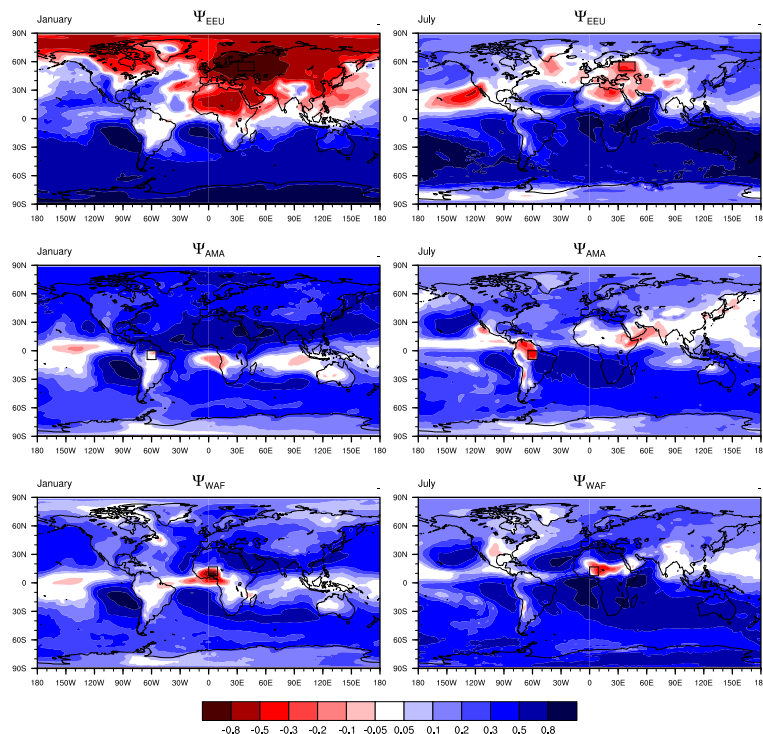


Fig. 7. The degree to which moisture originating from the regions EEU (Ψ_{EEU} , top), AMA (Ψ_{AMA} , middle), and WAF (Ψ_{WAF} , bottom) is overrepresented in the upper half (positive values) or the lower half (negative values) of the atmospheric moisture column (Eq. 23), for January (left) and July (right). The results shown here are calculated for the 3-D-s variant; those for the 3-D-w variant are very similar (not shown).

[Title Page](#)
[Abstract](#)
[Introduction](#)
[Conclusions](#)
[References](#)
[Tables](#)
[Figures](#)
[◀](#)
[▶](#)
[◀](#)
[▶](#)
[Back](#)
[Close](#)
[Full Screen / Esc](#)
[Printer-friendly Version](#)
[Interactive Discussion](#)

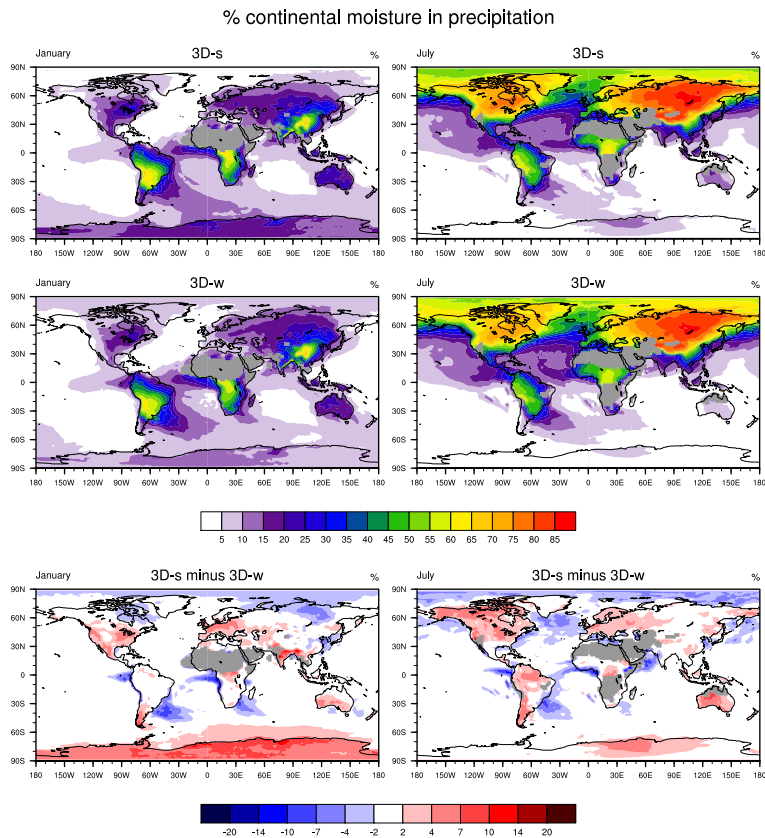


Fig. 8. The continental recycling ratio (R_c , % continental moisture in precipitation) as simulated with 3-D-s (top) and 3-D-w (middle), and the difference between the two (bottom), for January (left) and July (right). Grey areas are masked because less than five out of the ten years used for computing the averages have non-zero precipitation in the considered month, leading to statistically non-robust estimates.

Atmospheric water vapour tracers

H. F. Goessling and
C. H. Reick

Title Page

Abstract

Introduction

Conclusions

References

Tables

Figures



Back

Close

Full Screen / Esc

Printer-friendly Version

Interactive Discussion

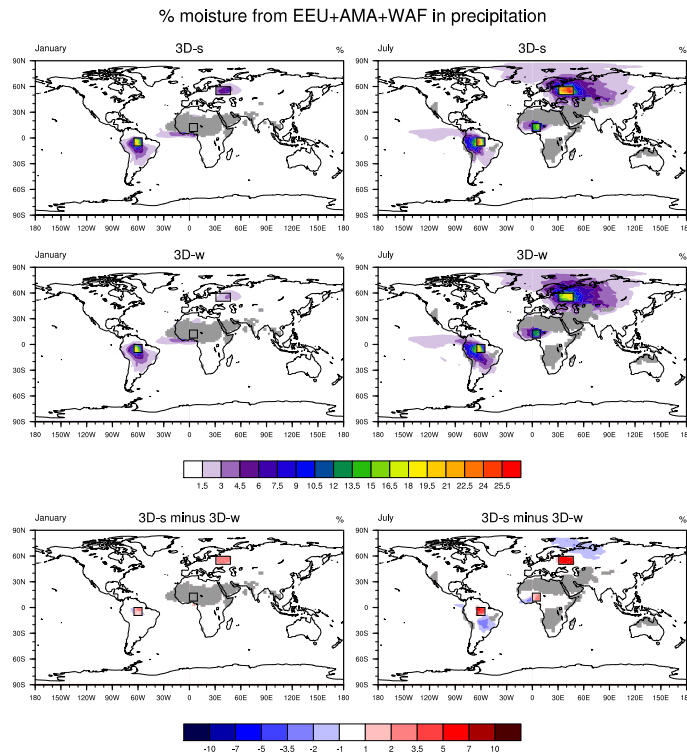


Fig. 9. The fraction of precipitation that originates from the rectangular source regions EEU, AMA, and WAF (black boxes) as simulated with 3-D-s (top) and 3-D-w (middle), and the difference between the two (bottom), for January (left) and July (right). Grey areas are masked because less than five out of the ten years used for computing the averages have non-zero precipitation in the considered month, leading to statistically non-robust estimates. Because the regions receiving significant amounts of precipitation from the three source regions are well separated, we took the liberty to show only the sum instead of the three individual plots.

Atmospheric water vapour tracers

H. F. Goessling and
C. H. Reick

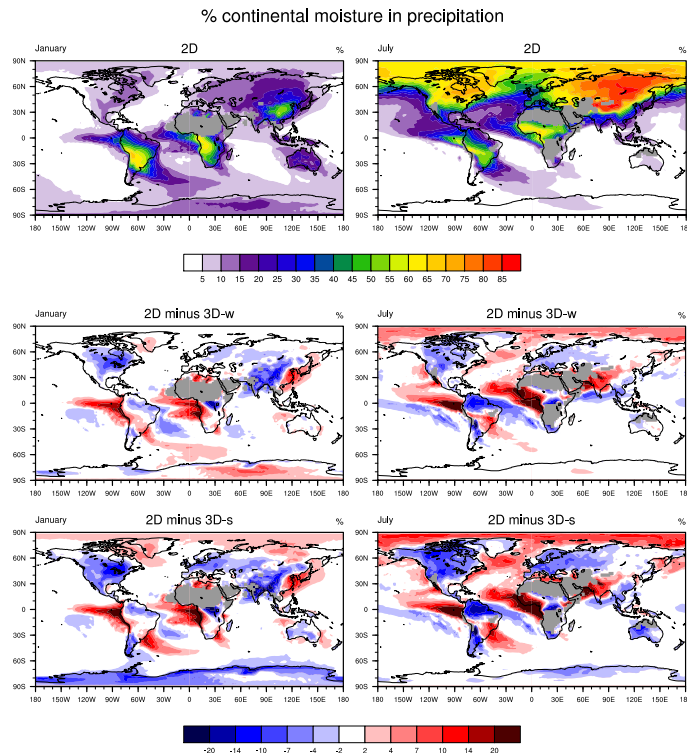


Fig. 10. Continental recycling ratios (R_c , % continental moisture in precipitation) as simulated with 2-D (top), and the difference between 2-D and 3-D-w (middle) and between 2-D and 3-D-s (bottom), for January (left) and July (right). Grey areas are masked because less than five out of the ten years used for computing the averages have non-zero precipitation in the considered month, leading to statistically non-robust estimates. Compare Fig. 8 for the absolute values of 3-D-s and 3-D-w.

Atmospheric water vapour tracers

H. F. Goessling and
C. H. Reick

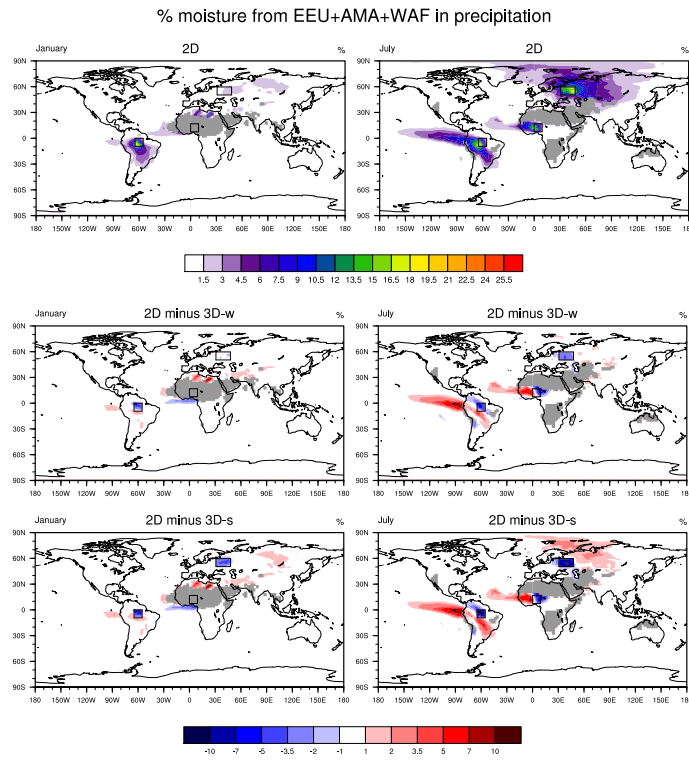


Fig. 11. The fraction of precipitation that originates from the rectangular source regions EEU, AMA, and WAF (black boxes) as simulated with 2-D (top), and the difference between 2-D and 3-D-w (middle) and between 2-D and 3-D-s (bottom), for January (left) and July (right). Grey areas are masked because less than five out of the ten years used for computing the averages have non-zero precipitation in the considered month, leading to statistically non-robust estimates. Because the regions receiving significant amounts of precipitation from the three source regions are well separated, we took the liberty to show only the sum instead of three individual plots.

[Title Page](#)
[Abstract](#)
[Introduction](#)
[Conclusions](#)
[References](#)
[Tables](#)
[Figures](#)
[Back](#)
[Close](#)
[Full Screen / Esc](#)
[Printer-friendly Version](#)
[Interactive Discussion](#)

Atmospheric water vapour tracersH. F. Goessling and
C. H. Reick

Title Page

Abstract

Introduction

Conclusions

References

Tables

Figures

◀

▶

◀

▶

Back

Close

Full Screen / Esc

Printer-friendly Version

Interactive Discussion

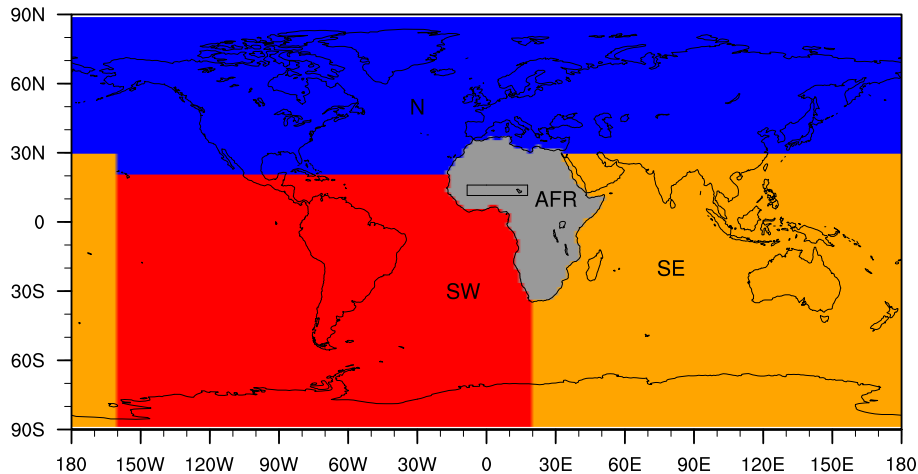


Fig. 12. The four evaporative source regions N (north), SW (southwest), SE (southeast), and AFR (Africa) that we use to determine the sources for precipitation in the Western Sahel region (black rectangle).

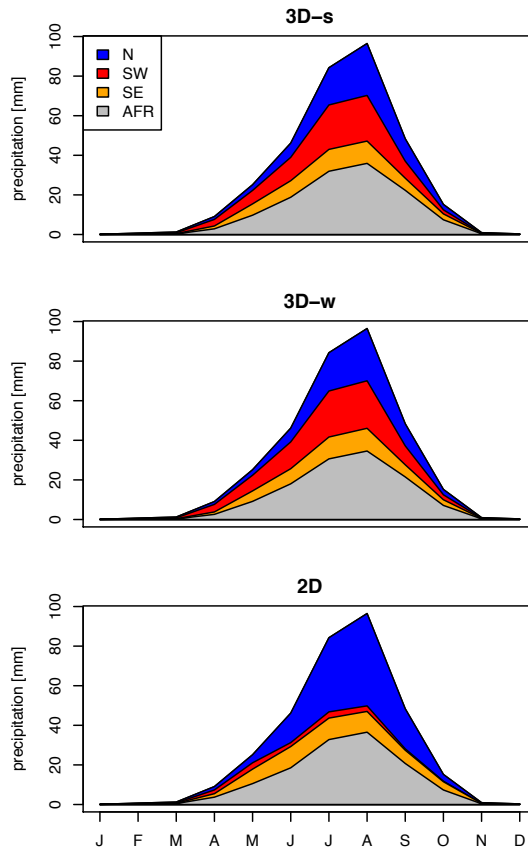


Fig. 13. Monthly absolute contribution to precipitation (mm) in the Western Sahel from the four evaporative source regions (compare Fig. 12) as determined by the moisture tracing variants 3-D-s (top), 3-D-w (middle), and 2-D (bottom).

Atmospheric water vapour tracers

H. F. Goessling and
C. H. Reick

Title Page

Abstract

Introduction

Conclusions

References

Tables

Figures

◀

▶

◀

▶

Back

Close

Full Screen / Esc

Printer-friendly Version

Interactive Discussion



Atmospheric water vapour tracers

H. F. Goessling and
C. H. Reick

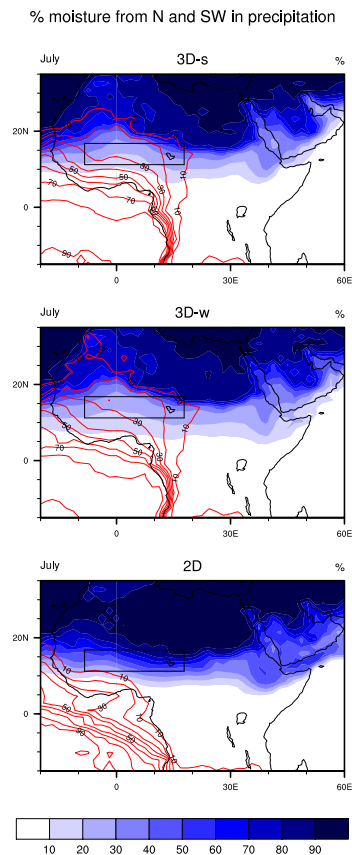


Fig. 14. Relative contribution to precipitation (%) in the Western Sahel (black rectangle) in July from the regions N (blue shading) and SW (red lines) (compare Fig. 12) as determined by the moisture tracing variants 3-D-s (top), 3-D-w (middle), and 2-D (bottom).

[Title Page](#)
[Abstract](#)
[Introduction](#)
[Conclusions](#)
[References](#)
[Tables](#)
[Figures](#)
[◀](#)
[▶](#)
[◀](#)
[▶](#)
[Back](#)
[Close](#)
[Full Screen / Esc](#)
[Printer-friendly Version](#)
[Interactive Discussion](#)

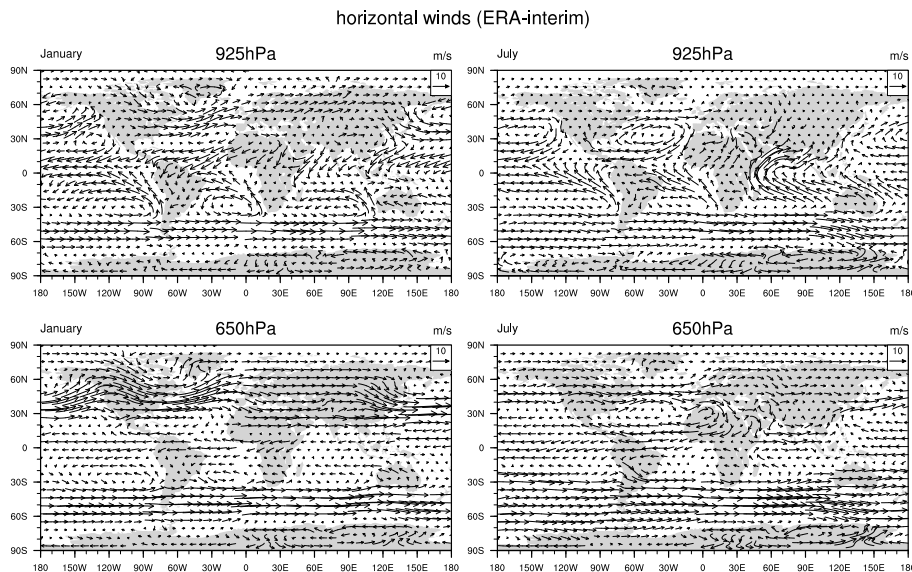

**Atmospheric water
vapour tracers**H. F. Goessling and
C. H. Reick

Fig. 15. Horizontal winds at 925 hPa (top, m s^{-1}) and 650 hPa (middle, m s^{-1}) from ERA-Interim reanalysis data (Dee et al., 2011) for January (left) and July (right), averaged over the years 2001–2010. Compare Fig. 3, top and middle.

Title Page

Abstract

Introduction

Conclusions

References

Tables

Figures

◀

▶

◀

▶

Back

Close

Full Screen / Esc

Printer-friendly Version

Interactive Discussion



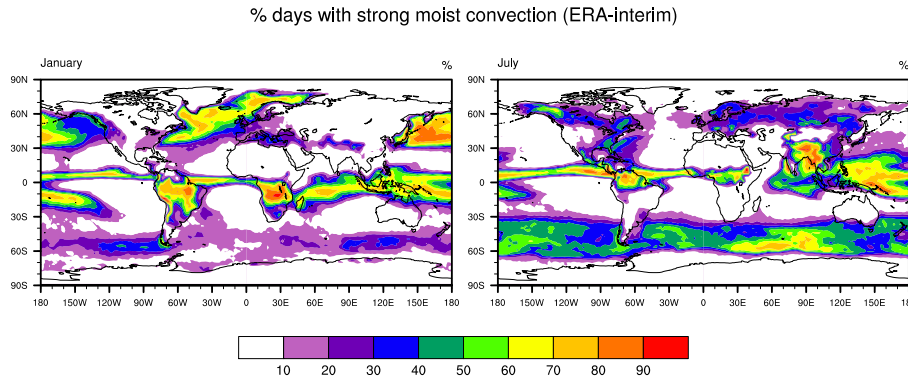
Atmospheric water vapour tracersH. F. Goessling and
C. H. Reick

Fig. 16. Fraction of days with strong moist convection from ERA-Interim reanalysis data (Dee et al., 2011) for January (left) and July (right), remapped to a T63 grid and averaged over the years 2001–2010, where we consider events as strong if the generated daily amount of convective precipitation exceeds 10% of the total column water content. Compare Fig. 2.

Title Page

Abstract

Introduction

Conclusions

References

Tables

Figures

◀

▶

◀

▶

Back

Close

Full Screen / Esc

Printer-friendly Version

Interactive Discussion

